NANOSTRUCTURED IRON OXIDE MODIFIED CONDUCTING PAPER FOR CANCER DIAGNOSTICS

to be submitted as Major Thesis in fulfilment of the requirement for the degree of

M. Tech (Industrial Biotechnology)

Submitted by

MOHAMMAD UMAR
(2K14/IBT/09)

Delhi Technological University, Delhi, India

Under the supervision of

Prof. B. D. Malhotra

Department of Biotechnology
Delhi Technological University
(Formerly Delhi College of Engineering)
Delhi-110042, INDIA

DECLARATION

Certified that the major thesis entitled **"Nanostructured Iron Oxide Modified Conducting Paper For Cancer Diagnostics ",** submitted by me is in fulfilment of the requirement for the award of the degree of Master of Technology in Industrial Biotechnology, Delhi Technological University. It is a record of original research work carried out by me under the supervision of Prof. B.D. Malhotra, Department of Biotechnology, Delhi Technological University, Delhi 110042. The matter embodied in this thesis is original and has not been submitted for the award of any other degree/diploma.

Mohammad Umar
2K14/IBT/09

CERTIFICATE

This is to certify that the M.Tech thesis entitled **"Nanostructured Iron Oxide Modified Conducting Paper For Cancer Diagnostics"** submitted by **Mohammad Umar (2K14/IBT/09)** in fulfilment of the requirement for the major thesis during M.Tech, Delhi Technological University (Formerly Delhi College of Engineering), is an authentic record of the candidate's own work which was carried out by her under my guidance. The information and data enclosed in this dissertation is original.

Prof. B. D. Malhotra
Department of Biotechnology
Delhi Technological University
Delhi – 110042

Prof. D. Kumar
Head of Department
Department of Biotechnology
Delhi Technological University

ACKNOWLEDGEMENTS

By the grace of almighty, I express my profound sense of reverence and gratitude to my mentor Prof. Bansi D. Malhotra, Department of Biotechnology, Delhi Technological University for giving me the opportunity to work in Nanobioelectronics laboratory, his valuable guidance, congenial discussion, incessant help, calm, endurance, constructive criticism and constant encouragement throughout this investigation right from the imitation of work to the ship shaping of thesis.

I am also immensely thankful to our Head of Department Professor D. Kumar and other faculty members for letting me carry out this work in the department.

I am highly indebted to Mr. Saurabh Kumar, Mr. Suveen Kumar, Ms Shine Augustine (PhD Scholar) and Dr. Chandra Mouli Pandey for their guidance and constant supervision as well as for providing necessary information regarding the instruments and experiments and also for their support in completing the report.

Lastly and most importantly I am thankful to my parents without whose constant support and guidance, I would never have been able to achieve any of this.

Mohammad Umar

2K14/IBT/09

CONTENTS

ABBREVIATIONS AND SYMBOLS

Ab	Antibody
BSA	Bovine serum albumin
CEA	Carcinoembryonic Antigen
CP	Conducting Paper
DMSO	Dimethyl sulphoxide
EIS	Electrochemical Impedance Spectroscopy
PBS	Phosphate buffer saline
PEDOT	Poly(3,4-ethylenedioxythiophene)
PSS	Polystryrene sulphonate
SEM	Scanning Electron Microscopy
TEM	Transmission Electron Microscopy
XPS	X-ray photoelectron spectroscopy
XRD	X-ray diffraction
$[Fe(\underline{CN})_6]^{4-/3-}$	Ferro-ferricyanide

LIST OF TABLES

LIST OF SCHEMES/FIGURES

Chapter 1

Abstract

Nanostructured iron oxide modified conducting paper for cancer diagnostics

Mohammad Umar

Delhi Technological University, Delhi, India
E-mail ID: umar.mnnit@gmail.com

1. ABSTRACT:

This dissertation contains results of the studies relating to the fabrication of a label-free, lightweight and flexible conducting paper based immunosensing platform comprising of poly(3,4-ethylenedioxythiophene):poly(styrenesulfonate) (PEDOT:PSS) and iron oxide nanocomposite for the detection of carcinoembryonic antigen (CEA), a cancer biomarker. The effect of various solvents such as sorbitol, ethanol, propanol, n-methyl-2-pyrrolidone (NMP) and dimethyl sulfoxide (DMSO) on the electrical conductivity of PEDOT:PSS coated whatman filter paper #1 (conducting paper, CP) has been investigated. Increment in the conductivity of the conducting paper electrode by two-fold was observed (from 6.84 x 10^{-4} to 2.40 x 10^{-2} S cm^{-1}) after treatment with DMSO (DMSO@CP). Further, the incorporation of iron oxide nanoparticles (nFe_2O_3) into DMSO@CP has enhanced the electrochemical performance and signal stability. Thereafter, biorecognition element anti-CEA was immobilized on the modified electrode surface (nFe_2O_3/DMSO@CP) for the detection of CEA and bovine serum albumin (BSA) was used for blocking of nonspecific sites. Electrochemical response studies indicated that this BSA/anti-CEA/nFe_2O_3/DMSO@CP electrode has a sensitivity of 10.2 μA ng^{-1} mL cm^{-2}, limit of detection 0.27 ng mL^{-1} with good linearity in the detection range 4-25 ng mL^{-1} and shelf life of 34 days. This fabricated immunosensor has also been validated via detection of CEA in serum samples of cancer patients employing ELISA technique.

Chapter 2

Introduction

2. INTRODUCTION:

Conducting paper based electronic devices are revolutionizing modern society by setting the trend of low-cost, flexible and portable and lightweight electronic devices, such as roll-up display, wearable gadgets, printed circuit boards, thin film transistors (TFTs), light-emitting diodes, paper batteries, and biosensing applications.(Manekkathodi *et al.*, 2010) In this context, conducting paper based electrochemical biosensors are attracting more attention as its 3-D hierarchical cellulose fiber network as well as interconnected porosity both aids in the conduction of electronic as well as ionic charge carrier which plays a vital role in communication with desired biomolecules. Cellulose fibers, being the key component of conducting paper, allow liquid to penetrate its hydrophilic fiber matrix. Hence, this makes conducting paper an effective matrix for biomolecule immobilization. Besides this, it offers several advantages such as low cost, mechanical flexibility, biocompatibility, disposability as well as environmental friendliness. These properties make them excellent alternative substrates with remarkable technological feature and commercial aspect against conventional substrates such as indium tin oxide, glassy carbon and gold electrodes which are rigid, brittle, cost, need expert handling and require high-temperature processing.

Many materials have been employed for fabricating conducting paper like graphene (Hyun W *et al.*, 2013), carbon nanotube (Wang L. *et al.*, 2009), metal (Gong S *et al.*, 2014), metal oxide (Mannekathodi *et al.*, 2010) and conducting polymer (Kumar *et al.*, 2016). The drawback of using metal and metal oxide material is that they get easily peeled off when the electrode is bent. Besides this, carbon nanotube and graphene requires complicated step for its fabrication. Among these materials, conducting polymer is getting substantial attention because it offers good conductivity, fine solution processability, environmental stability, and are inexpensive. These conducting polymers have conjugated π-electrons in their backbone structure. Overlapping of their partially filled molecular orbitals allows the formation of

delocalized molecular wave function causing a free movement of electrons throughout the lattice (Bloor and Movaghar, 1983). These properties cause them to display unusual electronic properties such as electrical conductivity, low energy optical transition, low ionization potentials, and higher electron affinities. Among the various conducting polymers, poly(3,4ethylenedioxythiophene):poly(styrenesulfonate) (PEDOT: PSS) has been considered to be a suitable choice for development of a conducting paper due to its homogeneous entrapment in/on paper using a simple dip coating method with enhanced stability. It also manifests relatively high conductivity and has been found to be the most stable conducting polymer currently available (Groenendaal *et al*, 2000; Kirchmeyer and Reuter, 2005). And it is one of the most commercially successful conductive polymers, has captured broad attentions since excellent features of its conductive state such as low band gap, superior electrochemical and thermal stabilities, high transparency and good quality films can be easily fashioned on various substrates by conventional solution processing method. (Jang *et al*, 2005; Briseno *et al*, 2006; Wu *et al*, 2007; Okuzaki *et al*, 2003; Ashizawa *et al*, 2005 and Yan *et al*, 2008). The conductivity of PEDOT:PSS can be manipulated by chemical modification of the polymer backbone via treating with different solvents (Kim *et al.*, 2002). Further, the incorporation of nanoparticles can enhance the performance of conducting paper biosensor. Nanostructured oxides of iron have aroused much interest as they exhibit attractive nanomorphological, biocompatible, non-toxic and catalytic properties (Figuerola *et al.*, 2010). These materials also display enhanced electron-transfer kinetics and strong adsorption capacity, providing suitable microenvironment for the immobilization of biomolecules and leading to better electron transfer and enhanced biosensing characteristics. Some of the problem using iron oxide nanoparticle is its monodispersity and irregular shape of these particles but this problem was solved by using iron-oleate as a precursor and oleic acid as capping agent which also helps to form a protective monolayer (Zhang et al. 2006). The use

of conducting polymer nanocomposites/nanoparticles could greatly improve diffusion since they have much greater exposed surface area and as a result of this, the basic characteristics of a biosensor like low detection limit get enhanced. The oriented microstructure and the high surface area also facilitate high biomolecule loading and hence highly sensitive detection is possible. Moreover, the relative stability is increased due to the efficient bonding of biomolecule on the transducer surface which improves reproducibility.

Cancer is a disease in which a group of abnormal cells grow uncontrollably disregarding the rules of normal cell division process, resulting in uncontrolled growth and proliferation. (Hejmadi 2010) These growth advantages are typically produced from a number of different genetic and/or epigenetic changes, which lead to the activation of oncogenes and the inactivation of tumour suppressor genes. When this proliferation is allowed to continue and spread, it can prove to be fatal. Currently, cancer is the leading cause of death in today's world accounting for about 8.2 million deaths in recent past with approximately 14 million new cases and this figure is expected to increase by 70% over the next two decade (WHO report, 2012). Carcinoembryonic antigen (CEA) is an important cancer biomarker for diagnosis and routine monitoring. It is widely used around the world as its abnormal pre- and postoperative serum level is related to the depth of tumor invasion, the prominence of lymph node metastasis, advanced UICC stage, and higher postoperative relapse and is being used commonly in routine hospital cancer detection method (Iles 2012). There are many conventional techniques are available at present time to detect CEA biomarker like radioimmunoassay (Szturmowicz *et al.*, 1995), fluoroimmunoassay (Yuan *et al.*, 2001), chemiluminescence immunoassay (Blackburn *et al.*, 1991), enzyme linked immuno-sorbent assay (ELISA) (Rosa and Kumakura 1995) but these techniques can be pretty time consuming, costly, invasive method and also need skilled personnel. In this

context, conducting paper based biosensor offer a number of advantages such as simplicity, high sensitivity, cost effectiveness, flexibility, and require low sample volume.

This report contains result of studies relating to development of a flexible, label free, light-weight and disposable electrochemical biosensor for CEA detection.

Chapter 3

Literature Review

3.1 Nanomaterials

Nanomaterials can be defined as materials having the dimension in the range of 1 - 100 nm scale. The increased interest in nanomaterials can be credited to their distinct characteristic properties regarding optical, magnetic and electrical from the bulk material. Nanomaterials of different shapes, sizes and composition have been developed intending to provide to specific research needs (Poole *et al.*, 2003). Nanomaterials based structures are classified as zero-dimensional (clusters), one-dimensional (nanofibers, rods, wires, tubes), two-dimensional (films, plates, networks) and three-dimensional (scaffolds) structures. Nanotubes, dendrimers, quantum dots and fullerenes are the most common type of nanomaterials (Pokropivny *et al.*, 2007). Unique properties at the nanoscale are due to increased surface area and quantum effects. The increased surface area to volume ratio lends greater chemical reactivity than their bulk forms. Advancement in nanomaterials has focused research on developing nanostructures with controlled morphologies.

The electrical and photoconductivity properties of nanotubes and nanorods have aroused much interest. The mechanism of electrical conductivity of nanomaterials an attribute of their size is complex and are classified into following categories: surface scattering, quantized conduction, coulomb charging and tunneling, widening of band gap and change of microstructures. Apart from the above mechanisms, reducing imperfections, structural defects and dislocations improve the electrical conductivity of nanomaterials and nanostructures (Cao 2004).

Nanomaterials have been known to show unique optical properties due to increased energy level spacing or quantum confinements arising from spatial confinement of electrons and holes and formation of electric dipoles and discrete electronic energy level in nanomaterials. Another phenomenon that takes place due to size reduction is surface plasmon resonance that is caused when the size of the metal nanocrystals is smaller than the

wavelength of incident radiation (Cao 2004). These prominent optical properties have found applications in solar cells, imaging, laser sensor, tumor detection, optical detector, photocatalysis and biomedicine.

One aspect of nanomaterials is their magnetic property, attributed to surface atoms, that is not known in a number of bulk materials. For example, gold and platinum are non-magnetic in bulk form but tend to show magnetic behavior in nanometer size. The Au and Pt nanoparticles have been reported to be magnetic. Ferromagnetic particles tend to switch polarization and become paramagnetic when reduced to nanometer size and are often referred to superparamagnetic particles. This magnetic property of nanoparticles has been exploited for biomedical applications such as hyperthermia (increasing body temperature), drug targeting/drug delivery, Nuclear Magnetic Resonance (NMR) imaging, magnetorelaxometry and with a future anticipated application in tumor detection and radiotherapy (Tartaj *et al.*, 2003).

3.2 Conducting Polymer:

Polymers can be described as large molecules or macromolecules having high molecular mass (103-107 g mol^{-1}), composed of repeating simple and reactive molecule known as monomers joined to each other by covalent bonds.

Traditionally polymers are regarded to be good electrical insulators. A new class of polymers has recently emerged known as conducting polymers. By having conjugated C=C delocalized π-electron backbone structures they exhibit unusual electrical and optical properties, low ionization potential and high electron affinity earlier observed particularly in inorganic systems. Delocalized molecular wave function caused by overlapping of molecular orbitals turn these polymers into intrinsically electrically conducting polymer. They have partially filled molecular orbital which causes free movement of electron throughout the lattice. (Bloor and Movaghar, 1983). Conducting polymers are electronically different from

all the usual inorganic crystalline semiconductors. The mechanism of carrier transport in conducting polymer is more similar to that of amorphous semiconductors (hopping transport) than crystalline semiconductors (band transport). The electronic phenomenon has been described by charge carriers (solitons, polarons and bipolarons) in these systems (Heeger, *et al.,* 1986). It has been found that the doping produces active sites (polarons) which enable the carriers (electrons & holes) to move from one site to another by hopping mechanism through these active sites. There various factors which determine the conductivity of conducting polymer like length of polaron, the conjugation length, the overall length of chain and by transfer of charge to adjacent molecules (Kroschwitz, 1988).

Interesting applications of conducting polymers are seen in solar cells, lightweight batteries, electrochromic devices and molecular electronic devices. They have broadened the likelihood for modification of surface of conventional electrodes providing new and exciting properties.

3.2.1 Poly (3,4-ethylenedioxythiophene):poly(styrenesulfonate)

PEDOT:PSS is a polymer mixture of two ionomers. The first component is poly(3,4-ethylenedioxythiophene) or PEDOT is a conjugated polymer which bears positive charges, the other component is made up of sodium polystyrene sulfonate which is a sulfonated polystyrene. Fraction of the sulfonyl groups are deprotonated and carry a negative charge. Collectively the charged macromolecules form a macromolecular salt.

Poly(3,4-ethylenedioxythiophene) is an electrochemically stable conjugated polymer which can be oxidized (doped) to a state of high electrical conductivity, while preserving reasonable transparency. PEDOT in the neutral state is opaque blue-black and is relatively transparent sky blue in the doped state. PEDOT itself is an insoluble material, but when it is chemically synthesized in the presence of poly(4-styrenesulfonate) (PSS), an aqueous

dispersion is obtained that can be cast into thin films. In this film, the PEDOT chains are incorporated into polyanionic PSS matrix to counterbalance the charges (Fig. 3.1). Thin aqueous films of PEDOT:PSS have been extensively utilized in a wide range of applications for example in antistatic coatings, as electrode in light-emitting diodes (LEDs), photovoltaics (PV), memories, sensors, and as active material for electrochromic devices, field-effect transistors and circuits in general (Nardes *et al.*, 2008).

The chemical structures of PEDOT and PSS are given in Fig. 3.1. PSS performs the dual function of charge balancing and stabilizing the aqueous dispersion. The consequence of this reaction is an odorless dark blue dispersion of two electrostatically bound polymers.

It also manifests relatively high conductivity and found to be the most stable conducting polymer currently available (Groenendaal et al. 2000 and Kirchmeyer and Reuter 2005).

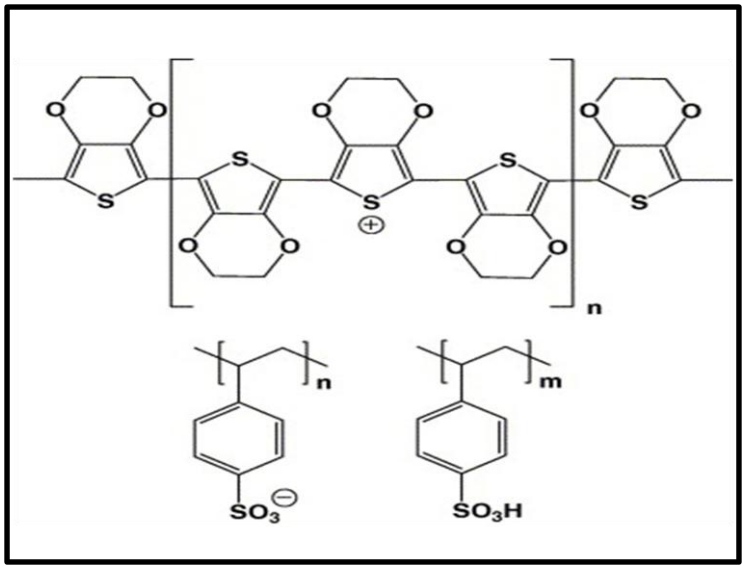

Figure 3.1: Structure of PEDOT:PSS

It also manifests relatively high conductivity and found to be the most stable conducting polymer currently available (Groenendaal et al. 2000; Kirchmeyer and Reuter 2005). Also, it is regarded as most commercially successful conductive polymer, has captured broad attentions since it has excellent features such as lower band gap, higher electrochemical

and thermal stabilities, high transparency and good quality films can be efficiently fashioned on various substrates by conventional solution processing method. (Okuzaki et al. 2003; Jang et al. 2005; Ashizawa et al. 2005; Briseno et al. 2006; Wu et al. 2007; Yan et al. 2008).

3.3 Biosensor:

A biosensor can be defined as a bioanalytical detecting device which converts a biological response into a measurable signal. When a specific target analyte interacts with the biological recognition entity, a signal is generated at the transducer proportional to the concentration of the analyte. Therefore, biosensors can measure compounds existing in the environment, chemical processes, food and human body at low cost when matched with classical analytical techniques. They provide the latest set of inexpensive, portable instrument that allows complex analytical measurements undertaken at decentralized locations rapidly.

It comprises of a biological recognition element closely associated with or integrated within a physicochemical transducer. When the biological element recognizes the target analyte, the corresponding biological responses are produced which are then converted into electrical signals with the help of transducer. The amplifier after receiving the small input signal from the transducer, provides a significant large output signal that carries the fundamental waveform features of an input signal. This amplified signal is then processed by the signal processor where it can later be stored, displayed and analyzed.

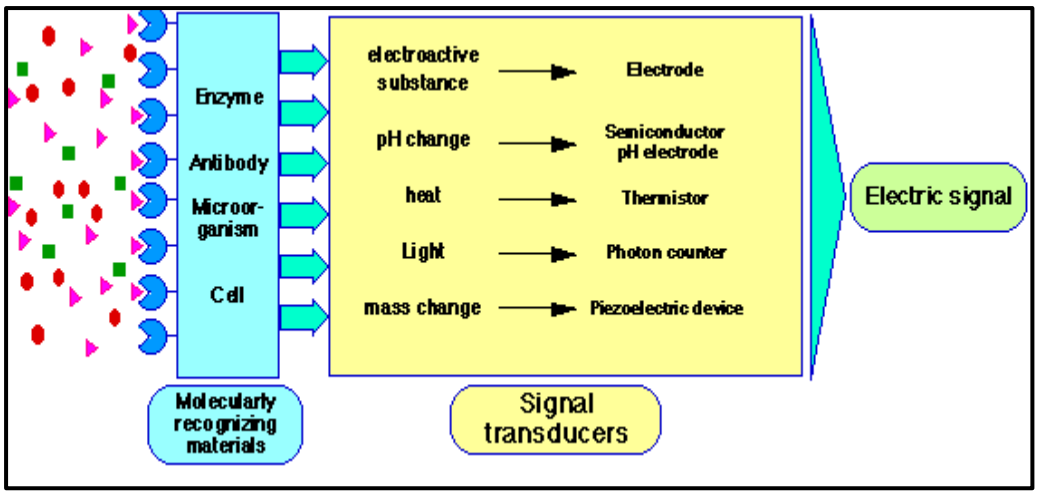

Figure 3.2: Schematic diagram of biosensor

3.3.1 Components of Biosensor:

3.3.1.1 Biomolecular recognition element:

They are an immobilized biological system or component that should be implemented as the receptor molecule which can specifically recognize the target molecule in a mixed population of several other biomolecules. They are very crucial for medical diagnosis as the sensitivity and specificity of the sensing molecules will perform a major role in the success of the sensor device. The following molecular recognition entities has been used for biomarker detection.

- **Biological materials** such as cells, tissue, microorganisms, cell organelles, cell receptors, enzymes, antibodies, nucleic acids, natural products etc
- **Biologically derived materials** such as recombinant antibodies, engineered proteins, aptamers etc
- **Biomimics** such as synthetic receptors, biomimetic catalysts, combinatorial ligands, imprinted polymers etc.

3.3.1.2 Transducer:

A transducer is a device that converts a molecular recognition signal event into a measurable electrical (often digital) signal such as current or voltage values that can be quantified, displayed, and analyzed. The output of the transducer can be displayed directly or can be further processed by a microprocessor or amplifier or other signal processing techniques. Some of the commonly used transducers in biosensing are:

Electrochemical (amperometric, potentiometric, conductimetric, impedimetric etc), **Optical** (surface plasmon resonance (SPR), fluorescence, interferometric), **Thermometric** (enzyme thermistor, thremal enzyme-linked immunosorbent assay etc), **Piezoelectric** (quartz crystal microbalance (QCM), surface acoustic wave devices), **Magnetic** (magneto resistive devices, paramagnetic labels etc), **Micromechanical** (resonating beam structures etc).

Among these transducers, electrochemical biosensors are found to be more suitable for onsite analysis and can function accurately with the turbid sample. Furthermore, they are very useful as they provide several advantages like fast detection, simple and inexpensive technique, high sensitivity and selectivity and easy miniaturization.

3.3.1.3 Amplifier and signal processor:

Amplifier is a standard electronic part which is employed to amplify the transducer signal before it is fed to the signal processor. The data is then converted by signal processor into concentration units and are transferred to a display or/ and data storage device.

3.4 Nanomaterial based biosensor:

There is an increased interest of nanomaterials in health care. Emergence of new materials and their composites have increased prospect for production of new biosensors capable of providing onsite results without needing skilled personnel or advanced machinery. At nanoscale, materials display novel properties that help to fabricate sensors with high sensitivity and fast analyte detection. Nanomaterials have been utilized for direct wiring of biological element to electrode surface to enhance the electrochemical reaction and for amplification of signal. Nanomaterials based biosensors use an an immobilized bioreceptor probe that is specific for the specific analyte molecules. Graphene, carbon nanotubes, nanowires, dendrimers, quantum dots and various nanocomposites are used for creating distinct novel sensors. Nanomaterials are transforming the field of biological and chemical analysis, to enable fast detection of multiple analytes *in vivo* by developing nanosensors, nanoprobes and other nanosystems. Among the nanomaterials, nanostructured oxides of metals (zinc, iron, cerium, tin, zirconium, titanium, metal and magnesium) have been found to exhibit interesting nanomorphological, functional biocompatible, non-toxic and catalytic properties. These materials also exhibit enhanced electron-transfer kinetics and strong adsorption capability, providing suitable microenvironments for the immobilization of biomolecules and resulting in enhanced electron transfer and improved biosensing characteristics. (Solanki *et al.*, 2011)

Luo *et al* have fabricated a highly conductive TiO_2 nanoneedle film as a support for the immobilization of cytochrome c to facilitate electron transfer between redox enzymes and electrodes. In this system, they found inherent enzymatic activity towards H_2O_2 released from human liver cancer cells. (Luo *et al.*, 2009) Feng et al reported the nanocomposite of CeO_2 and CH has been used to immobilize an ssDNA probe for colorectal cancer genes using

methylene blue as an indicator (Feng *et al.*, 2006). Wei *et al* reported an electrochemical immunosensor based on (iron oxide nanoparticles mixed with gold) Au-Fe_3O_4 nanoparticles have been used for the detection of the prostate-specific antigen (PSA) cancer biomarker. This nanomaterias modified sensor displays a wide linear range (0.01–10 ng/mL), low detection limit (5 pg/mL), good reproducibility and stability. (Wei *et al.*, 2010) Li et al reported a electrochemical immunosensor for the detection of prostate specific antigen (PSA) cancer biomarker has been developed based on dopamine (DA) functionalized Fe_3O_4 and using graphene sheet (GS) as sensing platform and ferrocene functionalized iron oxide (Fe_3O_4) as a label . This label was constructed by first anchoring dopamine (DA) on Fe_3O_4 surface followed by conjugating ferrocene monocarboxylic acid (FC) and secondary-antibody (Ab2) onto Fe_3O_4 through the amino groups of DA (DA-Fe_3O_4-FC-Ab2). The greatly enhanced sensitivity relies first on the amount of DA molecules anchored onto Fe_3O_4 increased the immobilization of F_C and Ab2 onto it which in turn increased the sensitivity of the immunosensor. And second, due to the large specific surface area of graphene sheet (GS) increased primary antibodies (Ab1) loading and its good conductivity magnified the detection sensitivity of FC. Utilizing the redox current of FC as signal, the immunosensor demonstrates higher sensitivity, wide linearity range (0.01–40 ng/mL), lower detection limit (2 pg/mL), good reproducibility and stability. (Li *et al.*, 2011) Li *et al* reported a nitrodopamine (NDA) functionalized iron oxide nanoparticles (NDA–Fe_3O_4) based electrochemical immunosensor has been developed for detection of the prostate specific antigen (PSA) cancer biomarker. Primary anti-PSA antibody (Ab1) and secondary anti-PSA antibody (Ab2) label was immobilized on NDA–Fe_3O_4. Label construction was done by first combining mediator thionine (TH) with NDA–Fe_3O_4 on the basis of amino groups present in NDA, and then the amino group of TH was used to immobilize horseradish peroxidase (HRP) and Ab2. Owing to the high measure of NDA attached to the Fe_3O_4 surface, the loading of antibodies as well

as mediator and enzyme onto NDA–Fe_3O_4 was increased considerably, which increases the immunosensor sensitivity. The fabricated immunosensor possesses a wide range of linear response (0.005–50 ng/mL), lower detection limit (4 pg/mL), good reproducibility and high stability. This immunosensor was then used to detect the PSA contents in serum samples with satisfying results. (Li *et al.*, 2011)

3.5 Cancer

Cancer is a group of diseases which causes cells to grow and proliferate abnormally in uncontrolled fashion disregarding normal cell division process. Normal cells are regularly subjected to signals that manage cell division, cell differentiation and cell death. Cancer cells develop a sort of freedom from these signals as shown in Fig 3.3, resulting in uncontrolled growth and proliferation. If this proliferation is allowed to proceed and spread, it can be fatal. In fact, about 90% of cancer-related deaths are due to tumor spreading-a process called metastasis. (Hejmadi, 2010). Modifications occur typically in three main categories of genes viz., (proto)oncogenes, tumor suppressor genes and DNA repair genes collectively add to the development of cancer genotype and phenotype that opposes the natural and inherent death mechanism(s) embedded in cells like apoptosis, coupled with dysregulation of cell proliferation incident.

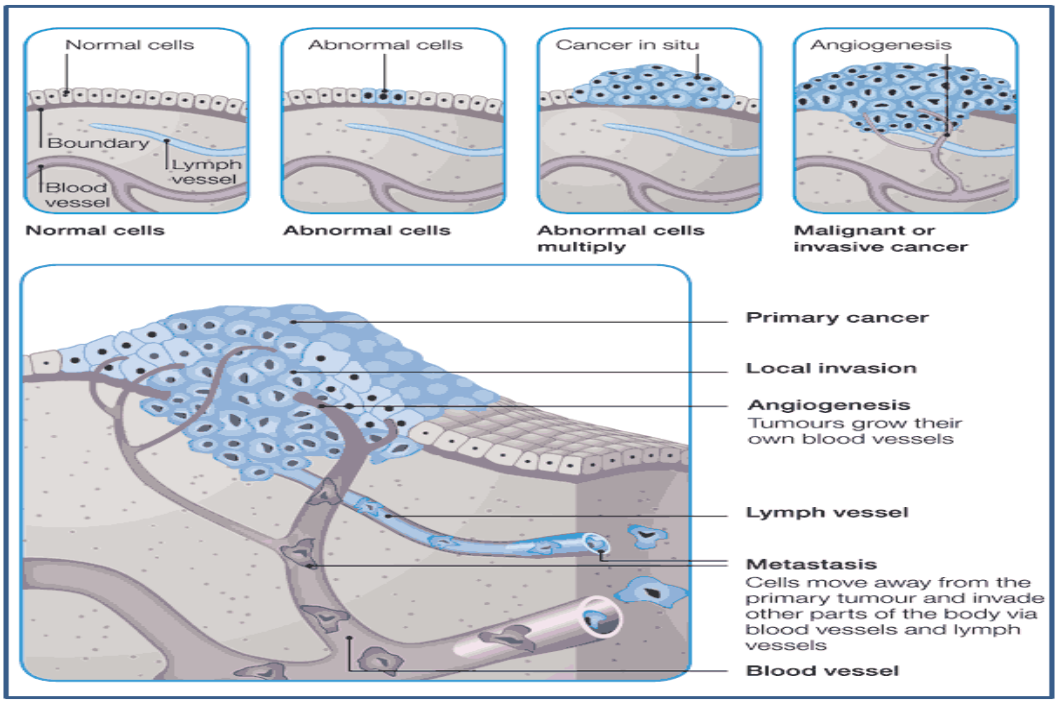

Figure 3.3: Cancer cell diagram

3.5.1 Biomarker:

A biomarker is a biomolecule found in blood, urine, or other bodily fluids, etc. that is measured and evaluated as an indicator that is used to assess normal biological processes, pathogenic processes, or pharmacologic responses. Biomarkers can differentiate an affected patient from a normal healthy person. These can also be used to locate the tumor and determine its stage, subtype, and response to therapy. Biomarkers are therefore invaluable means of cancer detection, diagnosis, patient prognosis and treatment selection. Diagnostic and prognostic biomarkers are quantifiable characteristics that help clinical oncologists interaction with the suspected patients. These mainly provide assistance in (i) identifying the at-risk person, (ii) early stage diagnosis, (iii) best treatment selection, and (iv) monitoring response to treatment. (Ludwig and Weinstein 2005)

Cancer Biomarkers

Many cancer biomarkers can be used to diagnose cancer at early stage like Cancer stem cells (CSCs), Human Papilloma Virus (HPV), Minichromosome maintenance (MCM) genes, mutations in the mtDNA, particularly in the D-loop region Oral fluid contains proteomic signatures, CA 19-9 (cancer antigen 19-9) or GICA (gastrointestinal cancer antigen), Prostate specific antigen (PSA), CA125, Alpha-foetoprotein (AFP), Adenomatous polyposis coli (APC) gene but among these carcinoembryonic antigen stand out as being the most widely used biomarker to detect cancer as its elevated levels are found in patients with colorectal, breast, lung, or pancreatic cancer, and also in smokers. Post-operative normalization of serum CEA level has been reported to be a favourable prognostic indicator in lung cancer and the identification of abnormal pre- and post-operative serum CEA levels may be useful in the auxiliary cancer prognosis or post-operative surveillance of colorectal cancer patients. (Wang *et al.*, 2007)

3.6.2 Carcinoembryonic antigen(CEA)

CEA is complex and highly glycosylated cell surface glycoprotein which is a subset of the tumor-associated antigens. The gene coding for CEA is classified as a member of the immunoglobulin supergene family. This family includes genes coding for adhesion proteins such as intercellular adhesion molecule 1 (ICAM-1) and lymphocyte function-associated antigen 1 as well as the major histocompatibility antigens. The human CEA gene family is found on chromosome 19q and contains 29 genes.

As mentioned above CEA is one of the most extensively used clinical tumor markers. The main reasons why CEA is useful as a serum tumor marker for colorectal and some other cancers are probably because CEA is a stable molecule, has a fairly restricted expression in normal adult tissue and is expressed at high levels in positive tumors. Furthermore, CEA

concentration in serum is also related to the state of tumor and used to identify recurrences after surgical resection. The normal range for CEA in an adult non-smoker is less than 2.5 ng/mL and for a smoker less than 5.0 ng/mL in human serum, but its level exceeds 100 ng/mL upon the development of certain cancers. (Lei *et al.*, 2013) A rising CEA level indicates progression or recurrence of cancer, which means that the detection of CEA in human sera samples can be employed to diagnose and monitor cancer at early stage.

3.6.3 Conventional Method for CEA detection:

A number of immunoassay methods including radioimmunoassay (Szturmowicz *et al.*, 1995), fluoroimmunoassay (Yuan *et al.*, 2001), chemiluminescence immunoassay (Blackburn *et al.*, 1991) and enzyme-linked immunosorbent assays (ELISAs) (Rosa and Kumakura 1995) have been employed in detecting serum CEA for clinical diagnosis. Despite the fact that these conventional methods provide accurate, reliable, sensitive detection of CEA, there are still some difficulties exist, such as utilization of radioactive elements, time-taking sample purification steps, incubation, washing steps before analysis and enzymatic reactions, the need of technical expertise as well as the requirement of specialized equipment.

3.6.4 CEA based Biosensor:

Carcinoembryonic antigen (CEA) is one of the most widely used tumor markers worldwide as its abnormal pre- and postoperative serum level observed significantly correlated with the depth of tumor invasion, the status of lymph node metastasis, advanced UICC stage, and higher postoperative relapse and is being used commonly in routinely in hospital for cancer detection. A biomarker test, to be of any clinical value, needs to be quick, simple to perform, inexpensive reliable and robust hence a CEA based biosensor can be developed so that the process of detection of cancer will become easy as it will simplify the

operation of detecting the cancer, it will also shorten the assay time, the cost of detection will be reduced and it can also be used in the fabrication of point of care device with no requirement of skilled personnel. (Iles, 2012)

3.6 Paper

The paper is a traditional material used for writing, printing, drawing and packaging. The potential use of paper transcending these simple and traditional means derives from its physical properties. The principal constituent of paper is cellulose fiber. Further, cellulose fibers can be functionalised, thus changing properties such as hydrophilicity, if desired, as well as its permeability and reactivity. (Liana *et al.*, 2012)

Paper-based platform technologies have built an exciting avenue in the area of POC diagnostics. They have the potentiality to change the pattern in developing the diagnostic assays, especially for the developing world because they are thin, light-weight, mechanically flexible, economical, renewable and are readily available across the world. These platforms are easy-to-fabricate, mass-producible, easy-to-use, and disposable. It can also absorb fluid samples within its hydrophilic fibre matrix without the requirement of an active pump or external source by capillary effect, and be incinerated for convenient and safe disposal. Therefore, these platforms present attractive strategies for developing affordable accessories with extensive applications such as drug development, water and environment quality evaluation and infectious diseases detection and biosensing in resource-limited settings. (Yager *et al.*, 2006)

3.6.1 Conducting Paper:

Traditionally papers are known to be non-conducting in nature as they are made of cellulose fibers. Nowadays, paper is made to have electrical conducting properties as they are thought to be providing new attire to existing technologies. Paper can be made conducting by various methods like by coating conducting polymer, impregnating carbon nanotubes, graphene, metal, metal oxide nanoparticle, etc.

Conducting paper based electrochemical biosensors are attracting more attention as its 3-D hierarchical cellulose fiber network as well as interconnected porosity both aids in the conduction of electronic as well as ionic charge carrier which plays a vital role in communication with desired biomolecules. Cellulose fibers, being the key component of conducting paper, allow liquid to penetrate its hydrophilic fiber matrix. Hence, this makes conducting paper an effective matrix for biomolecule immobilization. These bioanalytical paper electrode are becoming popular as they are flexible, easy portability, light-weight, wearable, inexpensive, disposable and environmental friendly. Fabrication of these hybrid technologies are on the way as there are numerous gadgets are now available such as roll-up display, wearable gadgets, printed circuit boards, thin film transistors (TFTs), light-emitting diodes, paper batteries, and biosensing application. (Manekkathodi *et al.*, 2010)

3.6.3 Nanomaterial modified conducting paper:

At the present time, a key limitation of paper-based electrochemical biosensors for the detection of low abundant biomarkers is the limited sensitivity.Therefore, by integrating paper with the ultra high surface area material, such as metallic nanoparticles and carbon based nanostructures, is still greatly required to improve the sensor sensitivity.

Zhao *et al*. fabricated a paper-based gold nanoparticle sensor which was able to detect the endonuclease which cleaves DNA, DNase I, as well as adenosine. This AuNPs transducer

proves to be cost-effective, low-volume, portable, disposable and easy-to-use colorimetric bioassays. The colorimetric determination was easy as paper provided bright background, and they were found to shield DNA-AuNP aggregates from nonspecific external stimuli (e.g., heat), which is ideal for long-term storage. Aggregation and disaggregation of AuNPs using controllable interparticle distances give visual readouts of the presence of various biological entities, which makes them ideal signal transducers for paper-based assays. Only small volumes (1 μL) of both DNA-AuNP aggregate probes and target sample solutions are required. (Zhao *et al*., 2008)

A paper based biosensor incorporated with nanocomposite of graphene (G), polyvinylpyrrolidone (PVP) and polyaniline (PANI) has been used for cholesterol detection. Electrochemical conductivity and hence sensitivity of the biosensor was amplified by the improved dispersibility of G which was due to the presence of small amount of PVP (2mgmL-1). Cholesterol oxidase (ChOx) was attached to G/PVP/PANI-modified electrode for the amperometric determination of cholesterol. A linear detection range of 50 μM to 10 mM with the limit of detection 1 μM was observed. This novel and sensitive paper- based biosensor is expected to become an alternative device for cholesterol diagnosis due to its simplicity, low cost, disposability and portability. (Ruecha *et al.*, 2014)

A PEDOT:PSS–CNT nanocomposite has been utilized for the fabrication of a conducting paper (CP) biosensor for cancer detection. Anti-carcinoembronic antigen (CEA) protein was immobilized for quantitative estimation of CEA, a cancer biomarker. This low cost, flexible and environmentally friendly conducting BSA/anti-CEA/CNT/FA@CP) paper electrode exhibits a high sensitivity of 7.8 mA (ng ml^{-1}) cm^2 and a linear range of 2–15 ng ml^{-1}. (Kumar *et al.*, 2015)

A flexible paper-based sensor was fabricated for the detection of ethanol. The glossy paper was used as the substrate, indium tin oxide (ITO) nanoparticulate powder as a sensing material and multi-walled carbon nanotubes as electrodes. The glossy paper was found to be a good alternative to filter paper due to the non-degradability and relatively smooth surface of the glossy paper and particularly while incorporating nanomaterials onto the surface rather than within the fibre matrix. (Arena *et al.*, 2010)

Therefore, there is an immense potential of nanomaterial modified conducting paper for biosensing application.

Chapter 4

Materials and Methods

4.1 Chemicals and reagents

PEDOT:PSS (1.3 wt%, PEDOT content 0.5 wt% , PSS content 0.8%), carcinoembryonic antibody (anti-CEA), CEA, Bovine serum albumin (BSA) were procured from Sigma Aldrich, India. DMSO was purchased from High Purity Laboratory Chemicals, Mumbai. Phosphate buffer saline (PBS, 50 mM, pH 7.0) containing ferri-ferro cyanide was made. Deionized water was obtained from Millipore water purification system which has been used in preparation of buffer and solutions. Whatman filter paper Grade 1 was procured from GE healthcare, UK. Oleic acid capped iron oxide nanoparticles (nFe_2O_3) were a gift.

4.2 Experimental:

4.2.1 Fabrication of paper electrode:

At first, 10 mg of nFe_2O_3 was doped into 10 ml of PEDOT:PSS solution and it was then ultrasonicated for 1 hour. It was found that nFe_2O_3 got dispersed without sedimention in PEDOT:PSS solution. Further, Whatman filter paper #1 (1 cm x 3 cm) was dipped for 1 hour into nFe_2O_3/PEDOT:PSS solution followed by drying in hot air oven at 100˚C for 10 minutes. Thereafter, the dried electrode was dipped in DMSO solution for 5 minutes and oven-dried at 120˚C for 5 minutes.

4.2.2 Fabrication of paper based biosensor :

Carcinoembryonic antibodies (20µl, 1000µg ml^{-1}) were immobilized on nFe_2O_3/DMSO@CP via the physiological adsorption. The electrode was then rinsed with phosphate buffer (PBS, 50 mM, pH 7.0) to remove any unbound antibodies. Again 0.1 %

BSA immobilization was done onto this paper biosensor electrode to block unspecific sites. After rinsing again with PBS, the electrode were stored at 4° C before carrying out the sensing studies. A schematic of the fabrication experiment is shown in Scheme 1.

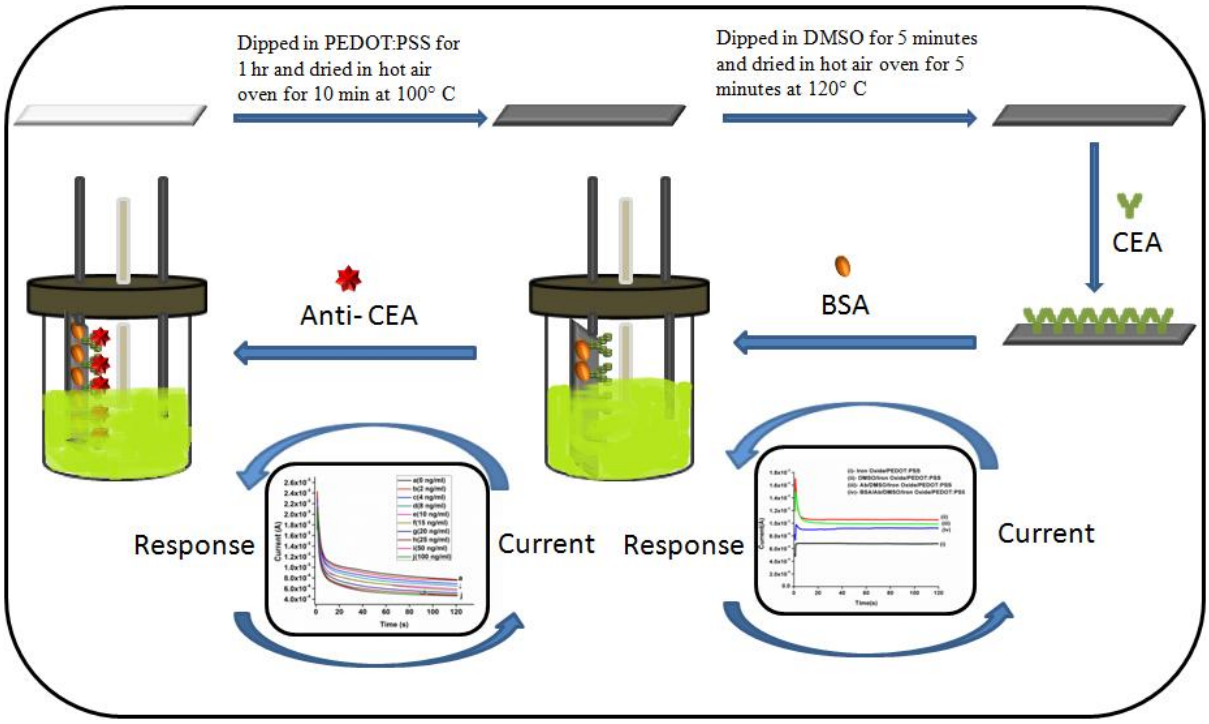

Scheme 1: Schematic representation of fabrication of cancer biosensor

4.3 Instrumentation:

4.3.1 Transmission electron microscopy (TEM):

Figure 4.1 TEM instrument

TEM is an instrument which operates on the same principle as light microscope but having greater resolving power than them as they use electrons as the light source instead of light and uses electromagnetic lens a to focus the electron beams. A beam of electrons passes through an ultra-thin sample it causes the scattering or disappearance of electrons depending on the density of the sample. A shadow image of the sample is formed which is magnified and focused onto the fluorescent screen or charge couple device (CCD) camera.

The interactions between the electrons and the atoms can be utilized to examine features like crystal structure and dislocations in structure and grain boundaries. Chemical analysis can also be performed. TEM has room for higher magnification which makes it an

invaluable tool in both medical, biological and materials research. In this work TEM (Tecnai G2 30, Ultratwin microscope) was used for characterization.

4.3.2 X-ray diffraction:

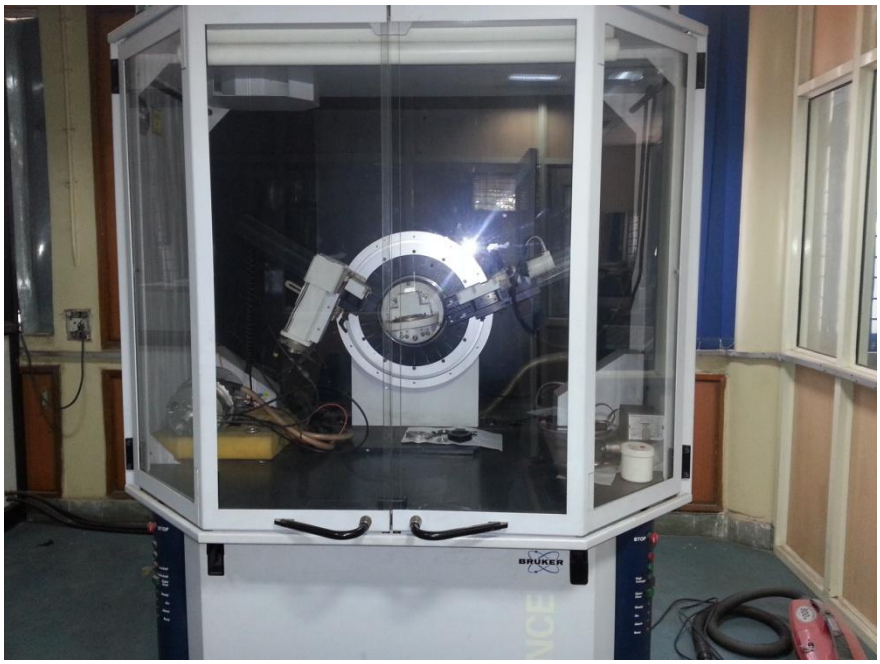

Figure 4.2: XRD instrument

X-ray diffraction analysis (XRD) is possibly the most extensively used analyzing technique for characterizing materials. When a focused X-ray beam interacts with planes of atoms, a part of the beam is diffracted. This diffraction of an X-ray beam is different for each crystalline solid material, depending on the arrangement and make up of atoms in the crystal lattice. Through X-ray diffraction technique we can measure the distances between the planes of the atoms by applying Bragg's Law equation given below

$$n\lambda = 2d \sin\theta,$$

where n is the order of the diffracted beam, λ is the wavelength of the incident X-ray beam, d (d-spacing) is the distance between adjacent planes of atoms , and θ is the angle of incidence of the X-ray beam.

The specific set of d-spacings which is produced by X-ray scanning, gives a unique "fingerprint" of the minerals present in the sample. When this is compared with standard reference patterns data it allows identification of the material. The characterization of the modified paper electrode was investigated via X-ray diffraction (XRD) studies (Bruker D-8 Advance). A monochromatic X-ray beam with Cu Kα radiation (λ = 1.5406 Å) was used to record the spectrum.

4.3.3 Four points probe system:

Figure 4.3 Four points probe system

Four points probe system is primarily used for measurement of resistivity of bulk and thin film specimen. It consists of four equally spaced tungsten metal tips and from the outer two tips a high impedance current is applied while a voltmeter measures the potential across the inner two tips which determine the resistivity of the specimen.

Resistivity can be obtained by using the following equation

$$\rho_0 = (V/I)\, 2\pi S \quad \text{..... Eq. 4.1}$$

Correction factor for thin films non-conducting bottom surface

$$G_7\,(W/S) = (2S/W)\, \log_e 2 \text{ .....Eq. 4.2}$$

Hence,

$$\text{Corrected } \rho = \rho_0 / G_7\,(W/S) \text{ .....Eq. 4.3}$$

where S = distance between equally spaced probe and W= width of slice

In this work, the conductivity measurement of various modified paper was done using four points probe technique with a low current source (LCS-02), digital microvoltmeter (DMV-001) and PID controlled oven (PID-200), SES Instruments, India.

4.3.4 Scanning electron microscope (SEM):

Figure 4.4: SEM instrument

A scanning electron microscope utilizes a focused beam of electrons to produce images of a sample by scanning its surface and magnifying the image with the help of electromagnetic field. When the beam of electron interact with atoms in the sample at various

depths, it produces signals that carry information about the sample's surface topography and its composition. In the most common or standard detection mode, the secondary electrons are emitted from the specimen surface. Consequently, SEM can produce image of very high-resolution of surface of sample, exhibiting finer details of less than 1 nm in size.

The detector collects these secondary electrons and the signal is amplified and displayed on a computer monitor. The resulting image generally is very simple to interpret, at least for topographic imaging of objects at low magnifications. The surface morphology was investigated by the scanning electron microscopy (Hitachi S-3700N)

4.3.5 X-ray photoelectron spectroscopy:

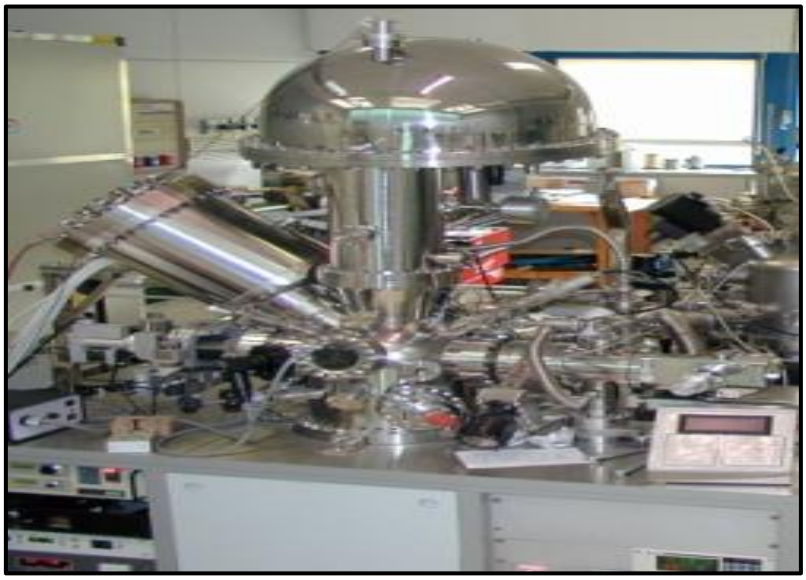

Figure 4.5: XPS Instrument

X-ray photoelectron spectroscopy (XPS) is a surface-sensitive quantitative spectroscopic technique which provides information about elemental composition, chemical state, empirical formula, and electronic state of the elements that are present in a material. It is based on the principle of photoelectric effect which refers to the emission of the electrons

from the sample surface in response to soft x-ray incident light. This incident light provides enough energy to electrons of the sample to get 'knocked' out from the sample surface producing electrons (photoelectrons) of discrete energy containing chemical information about the surface analyte. Surface analysis by XPS is achieved by analyzing the energy of the detected electrons. The spectrum obtained is a plot of number detected electrons per energy interval versus their kinetic energy. The kinetic energy of emitted electrons is given by:

$$KE = h\nu - BE - \Phi s \quad \text{..... Eq. 4.4}$$

where hν is the energy of the photon, BE is the binding energy of the atomic orbital and Φs is the spectrometer work function. This binding energy can be defined as the difference between the initial and final states when photoelectron leaves the atom. And since each element has a unique set of binding energies, hence, XPS can be used to identify elements upon the surface and determine their concentration. Changes in binding energy of element (chemical shift) arise due to differences in the chemical potential and the polarizability of compounds. With the help chemical shifts, chemical state of materials can be identified. In this work, X-ray photoelectron spectroscopy (XPS) (Scienta ESCA 200) was used.

4.3.6 Chronoamperometry:

Chronoamperometry is an electrochemical technique wherein a step potential is applied at working electrode and steady state current due to faradaic process occurring at the electrode is measured in a quiet unstirred cell as a function of time. This technique can determine diffusion constant and can be useful in studying kinetics and mechanisms. During this process, transfer of analyte occurs from the solution of higher concentration towards electrode surface which is controlled by a diffusion layer that is formed between the surface of electrode and solution. Due to the electron transfer events, a decay in the Faradaic current

is observed as described by the Cottrell equation. This decay is very slow than the charging decay in most electrochemical cells, cells with no supporting electrolyte are notable exceptions. This technique most commonly studied with a three electrode system. Since the current is integrated over relatively longer time intervals, chronoamperometry technique gives a better signal to noise ratio in comparison to other amperometric techniques.

Cottrell equation can be used to describe the current at any time following a large potential step in reversible redox reaction as a function of $t^{-1/2}$. It defines the current-time dependence for linear diffusion control at an electrode.

$$i = nFAC_0 (D_0/\pi t)^{-1/2} \quad \text{Eq. 4.5}$$

where n = stoichiometric number of electrons involved in the reaction, F = Faraday's constant, A = electrode area, C_0 = concentration of electroactive species and D_0 = diffusion constant of electroactive species.

4.3.7 Electrochemical Impedance Spectroscopy (EIS):

Electrochemical impedance spectroscopy (EIS) is a non-destructive, relatively new technique for the characterization of electrode interfaces and electrical properties of materials. This highly sensitive technique is capable of detecting small changes occurring at the electrode surface which may be of the order of a few Å. Thus, it is highly suited for the detection of biomolecules and their interaction occurring at the electrode surface.

EIS measures the change in the impedance of a stationary electrode in response to the application of periodic small amplitude AC signal at different frequencies (Kongsuphol *et al*., 2014). The frequency of the signal usually varies between 10^{-4} to 10^{6} Hz. The complex plane plots are commonly referred to as Nyquist plots or Nyquist diagrams enables easy prediction

of circuit parameters. Circuit parameters (R, C or/and L) are correlated to the electrode-electrolyte interface using 'equivalent circuit models.'

One of the most common equivalent models used for aqueous electrolyte system is the Randles' equivalent circuit. It consists of a series connection of bulk solution/electrolyte resistance (R_s or R_b) to impedance of the electrode-electrolyte interface. This impedance comprises of the resistance offered by the electrode surface to flow of electrons (R_{ct} or R_{et}) connected in parallel to the capacitance of the double layer formed at the electrode-electrolyte interface (C_{dl}). The mathematical representation of this circuit is given by the following equation –

$$Z(\omega) = R_s + 1/(1/R_{ct} + j\omega C_{dl}) \quad \text{..... Eq. 4.6}$$

The real and imaginary impedances (Z_{re} and Z_{im}, respectively) are given by the following equations –

$$Z_{re} = R_s + R_{ct}/(1 + \omega^2 R_{ct}^2 C_{dl}^2) \quad \text{..... Eq. 4.7}$$

$$Z_{im} = R_{ct}^2 C_{dl}\omega/(1 + \omega^2 R_{ct}^2 C_{dl}^2) \quad \text{..... Eq. 4.8}$$

The double layer at the electrode-electrolyte interface is formed due to non-specific adsorption of oppositely charged ions and other molecular species at the electrode surface. The double layer capacitance (C_{dl}) can be roughly estimated as the maximum value of Z'' in the Nyquist plot. The charge transfer resistance, or R_{ct} is the characteristic of the electrode surface and is easily affected by any change (e.g., adsorption, desorption, etc.) occurring at the electrode surface. It is mathematically related to the heterogenous electron transfer rate, k˚ by the following equation –

$$R_{ct} = RT/F^2\, k°C \quad \text{..... Eq. 4.9}$$

where, R is the molar gas constant, T is the temperature, F is the Faraday constant and C is the concentration of the electroactive species. The electrochemical studies were carried out by an Autolab Potentiostat/Galvanostat (Metrohm, Netherlands) using a conventional three-electrode cell with the BSA/anti-CEA/nFe2O3/DMSO@CP as working electrode, platinum as auxiliary electrode and Ag/AgCl as the reference electrode in phosphate buffer saline (PBS, 50 mM, pH 7.0) containing 5mM $[Fe(CN)_6]^{3-/4-.}$

Figure 4.6: Electrochemical analyzer

Chapter 5

Results and Discussion

5.1 Transmission electron microscopy (TEM) studies

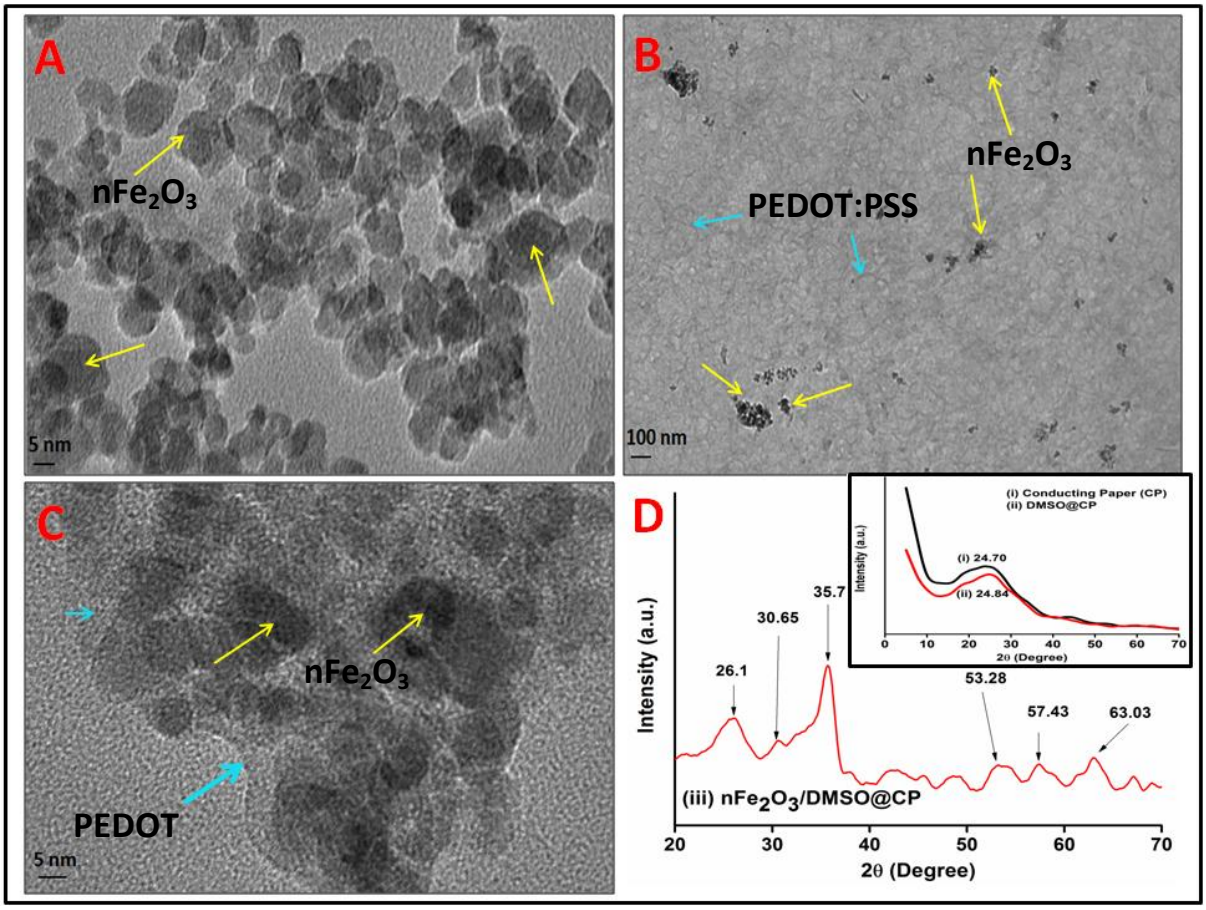

Figure 5.1: TEM image of (A) nFe_2O_3, (B) nFe_2O_3/PEDOT:PSS composite, (C) enlarge view of nFe_2O_3/PEDOT:PSS composite and (D) XRD pattern of (iii) nFe_2O_3/DMSO@CP and the inset showing XRD of (i) CP and (ii) DMSO@CP

The transmission electron microscopy image [Figure 5.1 (A)] shows that the oleic acid capped nFe_2O_3 are mono-dispersed and nearly spherical in shape having a particle size of 10–12 nm. In Figure 5.1(B) shows TEM image of nFe_2O_3/PEDOT:PSS.The nFe_2O_3 are found to be dispersed and embedded in PEDOT:PSS polymer. Further, the interaction between PEDOT:PSS and nFe_2O_3 interface has been examined with the help of TEM image [In figure 5.1(C)] PEDOT is seen encapsulating nFe_2O_3. The reason being that oleic acid capped nFe_2O_3 has a negative charge and PEDOT being a positive moiety, results in the electrostatic adsorption of amorphous PEDOT polymer over nFe_2O_3. (Jeong *et al*., 2015)

5.2 X-ray diffraction studies:

X-Ray Diffraction studies were performed to confirm the presence of iron oxide nanoparticles and analysis of various modified paper. Figure 5.1(D) shows XRD patterns of PEDOT:PSS, DMSO treated PEDOT:PSS (DMSO@PEDOT:PSS) and iron oxide nanoparticles doped DMSO treated PEDOT:PSS (nFe_2O_3/DMSO@PEDOT:PSS). X-Ray diffraction pattern analysis of PEDOT:PSS shows a broad peak at $2\theta=24.70^{o}$ which is similar to that existing in literature .(Singh et al. 2008). This diffraction peak appears to have arisen due to PEDOT thiophene ring (π-π) stacking (Aasmundveit *et al.*, 1999). DMSO treated PEDOT:PSS shows peak shifting from $2\theta= 24.70^{o}$ to $2\theta=24.84^{o}$ which corresponds to increase in the interchain planar ring stacking and also there is a decrease in intensity might result from the rearrangement of crystalline domain orientation. (Ouyang *et al*., 2015). XRD of nFe_2O_3/DMSO@PEDOT:PSS shows peak shift from 24.70 to 26.10 which might be due to nFe_2O_3 entrapment to PEDOT:PSS polymer chain. Additional peaks at 2θ =30.65, 35.70, 53.28, 57.43, 63.03 corresponding to the (2 2 0), (3 1 1), (4 2 2), (5 1 1), (4 4 0) reflections match with the standard XRD pattern of nFe_2O_3 (Powder Diffraction File, JCPDS No. 39–1346). (Singh *et al.*, 2008)

5.3 Electrical conductivity studies

The PEDOT:PSS coated paper (Conducting paper, CP) shows an electrical conductivity of about 6.8×10^{-4} S cm^{-1}. The effect of different solvents on electrical conductivity of CP has been shown in Table 1.The conductivity of CP was improved (6.8×10^{-4} to 1.92×10^{-2} S cm^{-1}) greatly in case of DMSO (DMSO@CP) and hence it was chosen for further studies. The reason for this increase in conductivity after DMSO treatment is because insulating PSS is largely removed and thus there is less coulomb interaction between PEDOT and PSS which causes the reorientation of the polymer enhancing the mobility of

charge carrier (Ouyang *et al.*, 2004). DMSO being an aprotic solvent forms hydrophobic bond with hydrophobic and conducting PEDOT conjugating polymer and PSS is washed away with distilled water. (Chou et al., 2015) Whereas, PEDOT:PSS doped with iron oxide nanoparticles after treatment with DMSO shows electrical conductivity of 2.40 x 10^{-2} S cm^{-1} which is more or less similar to DMSO@CP.

Table 1: Effect of various solvents on the electrical conducitivity of conducting paper.

Sr. No.	Sample	Conductivity (S/cm)
1	PEDOT:PSS coated on paper, CP	6.84 x 10^{-4}
2	CP dipped in NMP	6.9 x 10^{-4}
3	CP dipped in Sorbitol	1.3 x 10^{-3}
4	CP dipped in Propanol	3.6 x 10^{-4}
5	CP dipped in Ethanol	9.7 x 10^{-4}
6	CP dipped in DMSO, DMSO@CP	1.92 x 10^{-2}
7	nFe_2O_3/DMSO@CP	2.40 x 10^{-2}

5.4 Flexibility Studies

Flexible nature of nFe_2O_3/DMSO@CP electrode is investigated by folding of electrode in -180° to +180° fashion as shown in Figure 5.2(a) wherein positive and negative angles reveal folding of the electrode in upward and download direction respectively. The result is plotted as relative conductivity [ratio of measured conductivity (σ_m) to the initial conductivity (σ_o), σ_m/σ_o] against the folding angle. Figure 5.2(b) shows deviation in relative conductivity of nFe_2O_3/DMSO@CP electrode up to 17% by folding. Thus, it can be stated that the electrodes are flexible and there is less variation in conductivity observed after folding.

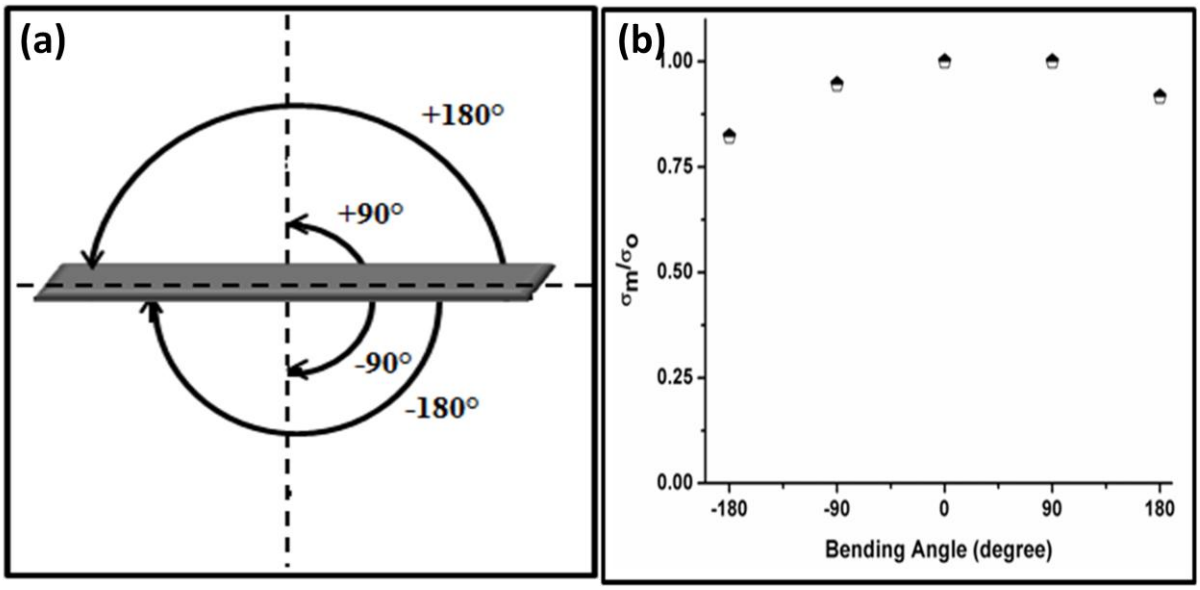

Figure 5.2 (a): Schematic diagram of electrode folding at different angle. **Figure 5.2 (b):** shows plot of relative conductivity vs bending angle.

5.5 Scanning electron microscopy (SEM) studies:

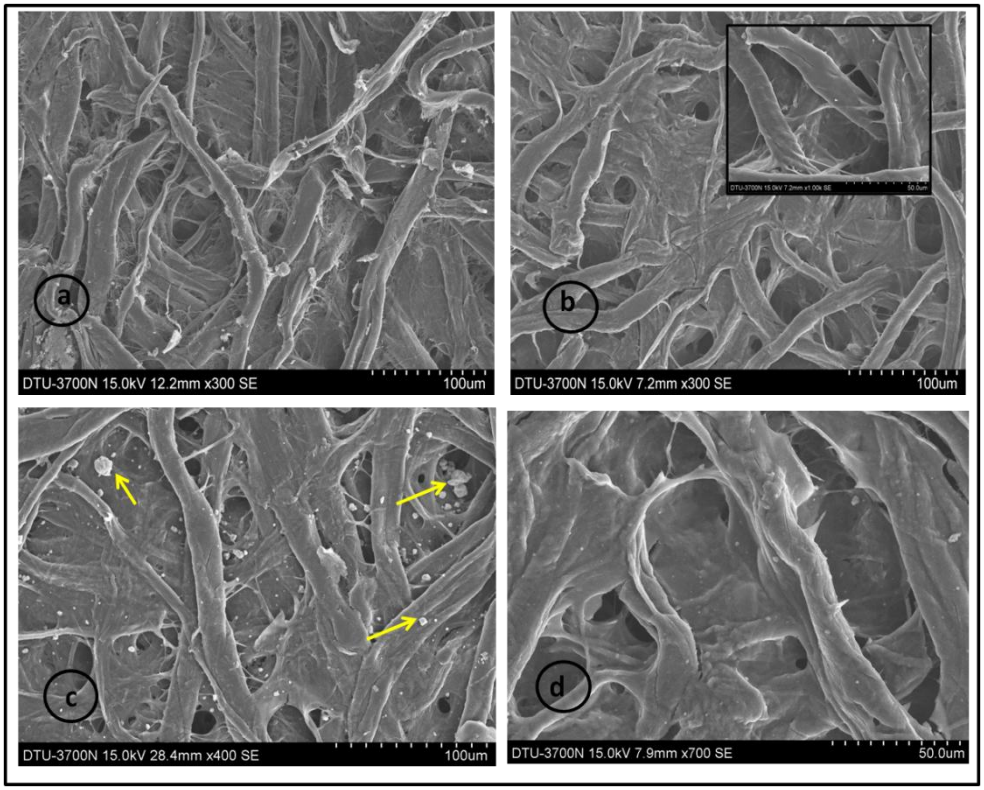

Figure 5.3: SEM image of (a) Whatman filter paper, (b) CP, (c) nFe_2O_3/DSMO@/CP, (d) anti-CEA/ nFe_2O_3/DSMO@/CP.

With the help of Scanning Electron Microscope surface morphology of the various modified paper was examined. In Figure 5.3 (a) cellulose fibers of Whatman paper can be seen clearly. And in Figure 5.3 (b) PEDOT:PSS is seen uniformly coated on paper which has somewhat smoothened the cellulose fiber. PEDOT:PSS is mainly adsorbed into paper fiber through capillary action because of high porosity and tiny interfiber air spaces present in paper. In Figure 5.3 (c) shows small spherical moiety of nFe_2O_3 embedded in the polymer structure of conducting paper. Figure 5.3 (d) Immobilization of antibodies has filled up the pores present in nFe_2O_3/CP. Further, shiny appearance on the paper electrode due to the build up of static charge confirms the immobilization of antibodies.

5.6 X-ray Photoelectron Spectroscopy (XPS) studies:

XPS studies were carried out to obtain chemical information of various modified paper electrode. Figure 5.4 shows wide scan XPS of (a) Conducting Paper (CP), (b) DMSO@CP and (c) nFe_2O_3/DMSO@CP. In all three spectra, the characteristic peaks observed at 168, 284 and 532 eV corresponds to S2P, C1S, and O1S respectively. However in third spectra an addition peak is observed at 727 eV which confirms the presence of nFe_2O_3.

The S (2p) core level spectra of PEDOT:PSS and DMSO treated PEDOT:PSS shown in Figures 5.5 (a) reveals two signature peaks. Each peak involves contributions from a spin-split doublet, S $2p_{3/2}$ and S $2p_{1/2}$ due to spin-orbital splitting of the sulfur atom. The S 2p contribution peaks at 163.42 eV and 165.80 eV corresponds to sulfur atoms of the PEDOT and those at higher binding energies at 167.39 eV and 168.86 eV belong to PSS because of the electronegative oxygen attached to a sulfur atom in the sulfonate group of the PSS. It can be noticed in Figure 5.5 (a) that the contribution in the peak intensity of S 2p from the PEDOT moiety has significantly increased, and that of PSS was reduced upon treatment with

DMSO. The ratio of PEDOT/PSS is increased from 0.52 to 0.69 after DMSO treatment. This increase can be attributed to the increase in the contribution of the PEDOT component to the signal. Moreover, there is a shift in the peak of PEDOT from 165.80 eV to 165.20 eV exihibits rearrangement in PEDOT structure.

Furthermore, the O 1s spectra in Figure 5.5 (b) exhibits peaks at around 533 and 531.27 eV, assigned to PEDOT and PSS moieties, respectively. The peak at 531.27 eV is due to oxygen atoms in double bond to the sulfur atoms in the PSS chain, and the peak at 533 eV correspond to oxygen atom from PEDOT chain. The peak intensity due to the PEDOT moiety also likewise increased after treatment with DMSO. PEDOT/PSS peak intensity ratio were calculated by the peak area of O1s spectra and is found to increase from 0.39 and 0.79 after DMSO treatment.

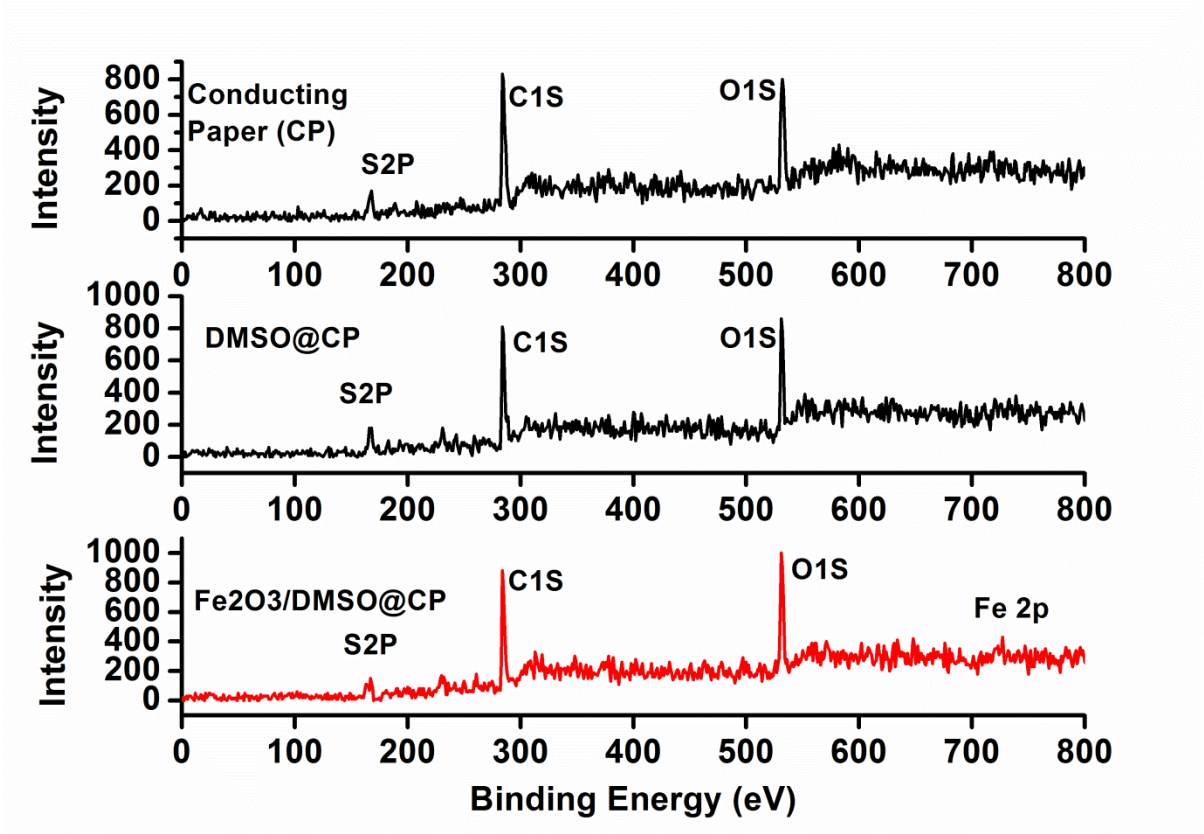

Figure 5.4: XPS survey scan of (a) Conducting Paper (CP), (b) DMSO@CP and (c) nFe2O3/DMSO@CP.

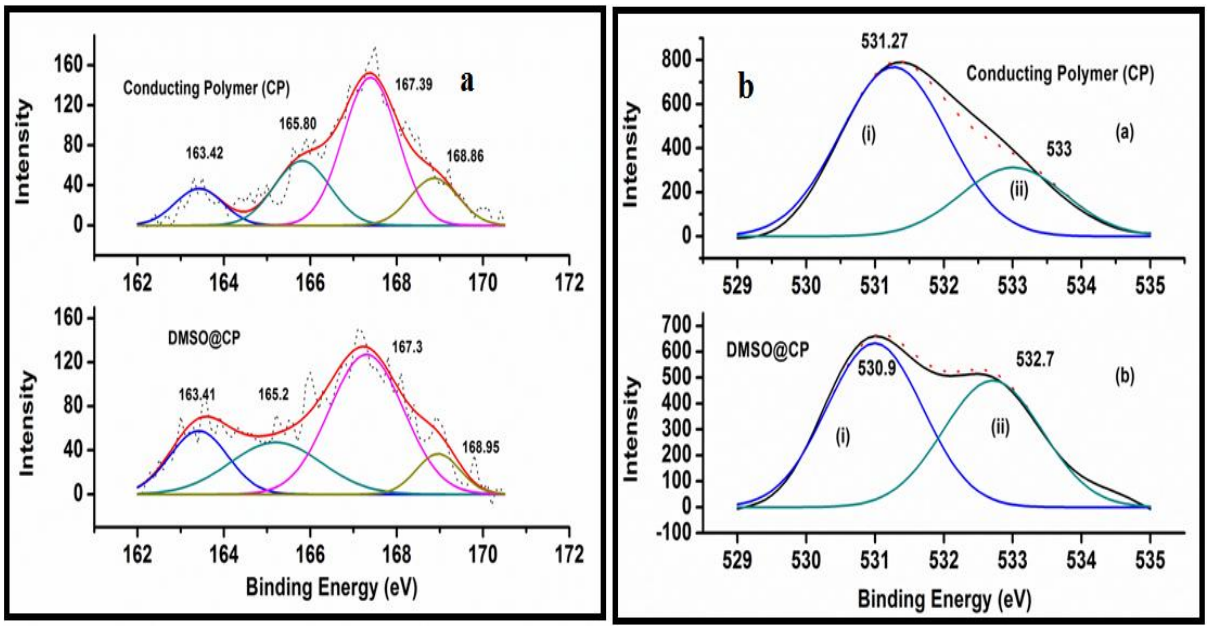

Figure 5.5: XPS deconvulation of a) S 2p and b) O 1s

5.7 Electrochemical studies:

Chronoamperometric study was conducted on an Autolab machine at a constant voltage of 2V at every 0.1sec. Figure 5.6a shows results obtained for (i) iron oxide nanoparticles doped CP, nFe_2O_3/CP, (ii) DMSO treated iron oxide nanoparicles doped CP, nFe_2O_3/DMSO@CP, (iii) anti-CEA immobilized over nFe_2O_3/DMSO@CP, anti-CEA/nFe_2O_3/DMSO@CP and (iv) BSA/anti-CEA/nFe_2O_3/DMSO@CP. Increase in electrochemical conductivity from ~0.65 mA to 1.06 mA after treating conducting paper with DMSO can be due to the removal of insulating PSS from the surface of conducting paper electrode. Decrease in electrochemical conductivity to a value 0.98 mA is due to blockage of electron transport sites on electrode surface due to immobilization of anti-CEA. Further, the decrease in electrochemical conductivity is due to blocking of more electron transport site due to BSA immobilization.

Electrochemical Impedance Spectroscopy (EIS) technique can be used to measure impedance by applying small amplitude alternating current and through which interfacial

property of electrode surface can be studied. Quantification of charge transfer resistance (Rct) of conducting paper electrode can be done by analyzing semicircle arc of Nyquist plot. Rct value of nFe_2O_3/CP is decreased from 966.39 Ω to 368.66 Ω [Figure 5.6 (b) and Figure 5.6 (c)] after treatment with DMSO which has shown to be the cause of removal of insulating PSS from the surface of conducting polymer and it also reduces columbic interaction between PEDOT and PSS. The increment in Rct 632.08 Ω [Figure 5.6 (d)] was observed after immobilization with anti-CEA as it masks surface available for charge transfer reaction. Further, the increase in Rct value to 892.18Ω is due to BSA immobilization, which cover up the unspecific sites therefore reduces the sites availability for charge transfer reaction. For understanding electron transfer kinetics, heterogenous electron transfer rate constant (Kct) is calculated by using Eq. 5.1

$$Kct = RT/(n2F2ARct[S]).. \text{ ..... Eq. 5.1}$$

where R is gas constant, T is absolute temperature, F is Faraday constant, A is electrode surface area (cm^2) , [S] is redox probe concentration (mol/cm^3) and n is number of electron transferred per molecule of redox probe. Kct value of nFe_2O_3/CP and DMSO treated nFe_2O_3/CP is found to be 5.51 $x10^{-4}$ and 14.45 $x10^{-5}$ respectively. Thus, treatment of conducting paper with DMSO is shown to increase electron transfer kinetics. Conductivity and electrochemical properties of different surfaces of modified paper electrode are shown in the table below.

Table 5.2: Electrochemical properties of modified surface electrode.

S.No.	Electrode Surface	Conductivity (Scm^{-1})	R_{ct}	R_s	K_{ct}
1	PEDOT:PSS on Whatman filter paper [Conducting Paper (CP)]	6.84×10^{-4}	2.30 kΩ	2.16 kΩ	2.32×10^{-5}
2	nFe_2O_3/CP	9.3×10^{-3}	966.39Ω	2.12kΩ	5.51×10^{-5}
3	nFe_2O_3/DMSO@CP	2.30×10^{-2}	368.66Ω	1.10kΩ	14.45×10^{-5}

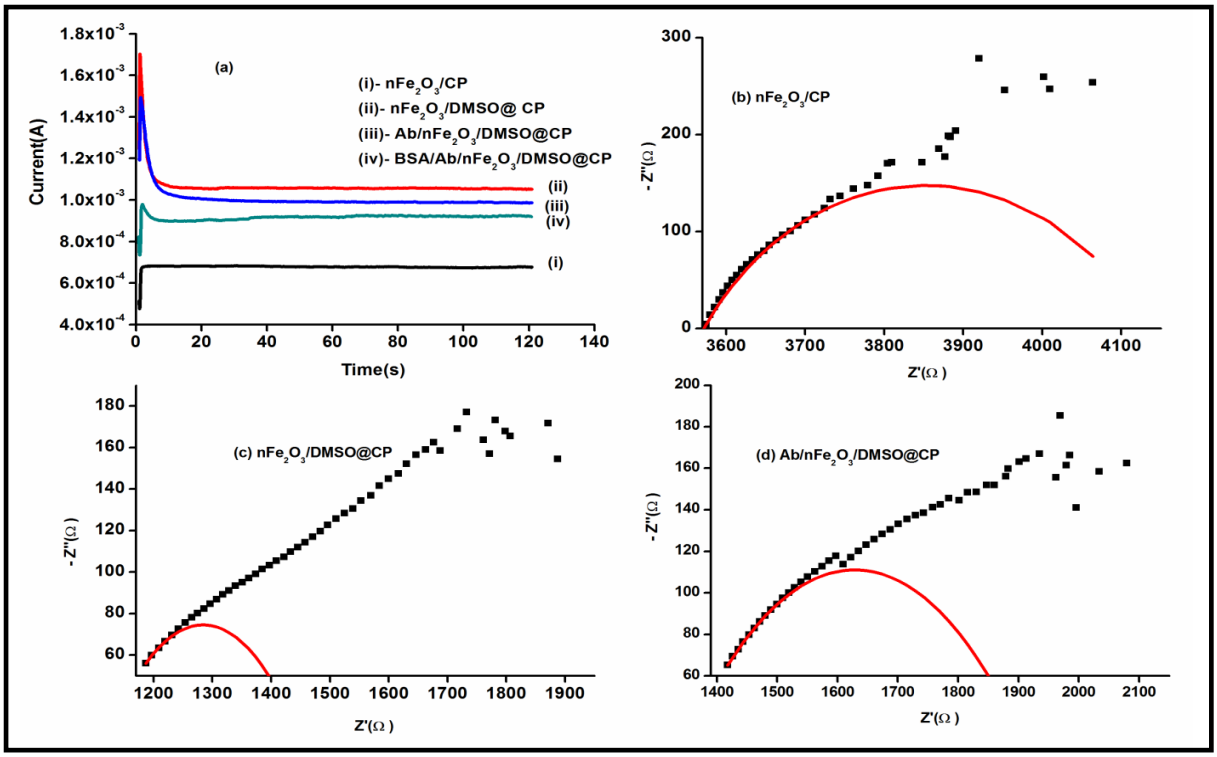

Figure 5.6: Characterization plot **(a)** Chronoamperometry plot , and EIS plot of **(b)** nFe_2O_3/CP, **(c)** nFe_2O_3/DMSO@CP EIS plot and **(d)** Ab/nFe_2O_3/DMSO@CP EIS plot

3.8 Electrochemical Response studies:

The response studies of BSA/anti-CEA/nFe2O3/DMSO@CP were recorded against increasing concentration of carcinoembryonic antigen (CEA) (2-100 ng/ml) in PBS (50 mM, pH 7.0) solution containing ferri/ferro cyanide after an incubation period of about 10 minutes. The response current was found to be decreasing with the increase in concentration of CEA due to building-up of immune complex onto the surface of electrode which blocks electron

transfer sites. Figure 5.7 (a) shows the sensitivity curve plotted between electrochemical response current and time. Limit of detection of 0.27 ng mL^{-1}, linearity range of 4-25 ng mL^{-1} is obtained with the sensitivity of 10.2 μA ng^{-1} mL cm^{-2} which follows equation below.

$$I\ (A) = -10.2\ \mu A\ mL\ ng^{-1} \times [CEA\ concentration] + 746\ \mu A;\ R^2 = 0.95 \quad \text{Eq. 5.2}$$

3.9 Control and Interference studies:

A control study was performed as shown in Figure 5.7 (c) to check the cross reactivity of the paper bioelectrode. An electrochemical current response was measured against the increasing concentration of CEA antigen for an electrode on which antibody was not immobilized. Since, there was no significant deviation obtained in electrochemical current response observed. Hence, the fabricated paper bioelectrode does not provide false response.

The selectivity study of this paper biosensor was investigated in the presence of cardiac troponin I (CTnI), endotheline-1 (Et-1) and cytokeratin-19 fragment (CYFRA) (2ng ml^{-1}). Figure 5.7 (d) shows there was no significant variation observed in current. However, a decrease in current was observed after addition of CEA (2 ng ml^{-1}) indicating high selective nature of the paper biosensor.

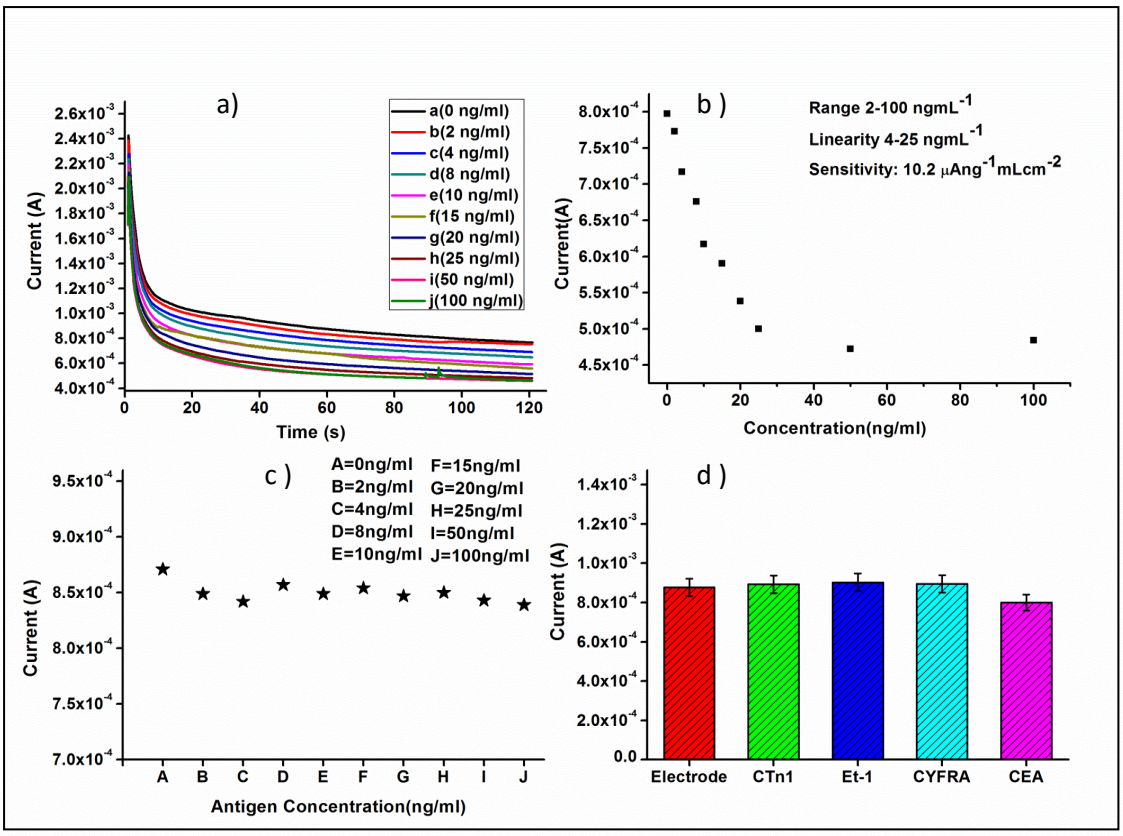

Figure 5.7: (a) Electrochemical response studies of BSA/anti-CEA/nFe_2O_3/DMSO@CP paper electrode obtained as a function of CEA concentration (2-100 $ngmL^{-1}$) using chronoamperometry **(b)** Calibration plot between the magnitudes of current recorded and CEA concentration **(c)** Control study plot **(d)** Interference plot

5.5 Reproducibility and Stability studies:

The electrochemical current response of five different electrodes having same surface area fabricated under a similar set of conditions was noted in the presence of CEA concentration (2ng/ml) [Figure 5.8 (a)]. The relative standard deviation of less than 5 percent (Mean Value = 802 µA) was observed which shows that this conducting paper electrode shows good reproducibility. Further, the experiments were repeated three times for each electrode and the error bars are included accordingly

Stability study experiment was conducted at the interval of three days to know the storage shelf life of the fabricated conducting paper biosensor electrode and result shows that after 34 days it still sustains electrochemical current response up to 82% respectively but after

37 days the electrochemical current response decreases up to 75%. Hence, it can be inferred that the fabricated electrode shows good stability up to 34 days as shown in Figure 5.8 (b).

5.6 Real sample analysis

Real sample analysis was done to evaluate the feasibility of the fabricated conducting paper biosensor electrode. The blood sample was collected from cancer patients and was processed at Rajiv Gandhi Cancer Institute & Research Centre (RGCI&RC) Rohini, Delhi, India. Ethical approval was obtained from Institutional Review board (No. RGCIRC/IRB/61/ 2014 and also from Institutional Ethical and Biosafety Committee, DTU (R.NO.:BT/IEBC/2014/714). The concentration of CEA in serum of cancer patients was measured at RGCI&RC using the VITROS CEA Reagent Pack and VITROS CEA Calibrators on the VITROS ECi/ECiQ Immunodiagnostic Systems, the VITROS 3600 Immunodiagnostic System and the VITROS 5600 Integrated System using Intellichecks Technology. A reasonable correlation can be seen exist between (a) CEA concentration in serum samples and (b) CEA concentration in synthetic samples. The result exhibits reasonable relative standard deviation (%RSD) indicating high accuracy of the conducting paper biosensor electrode as shown in Figure 5.8 (c)

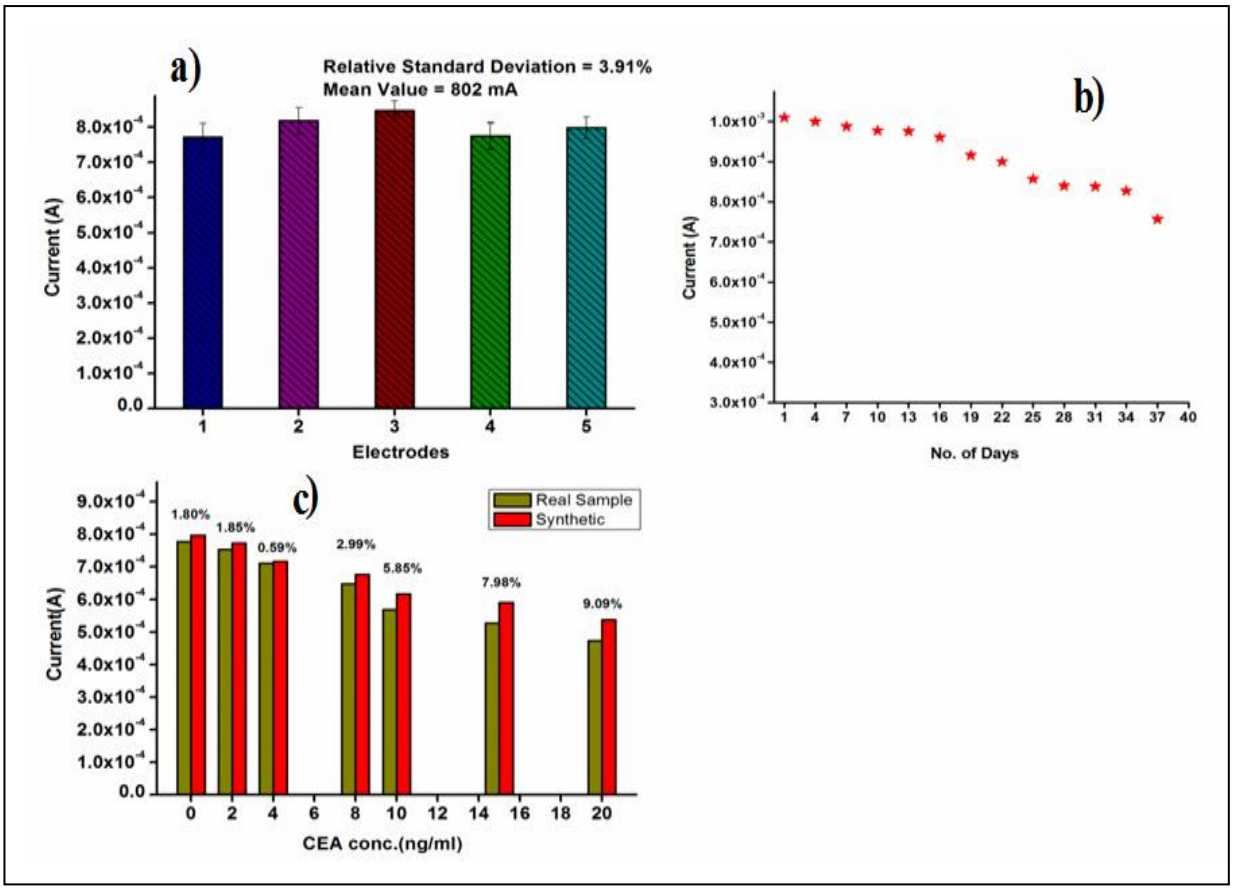

Figure 5.8: (a) Reproducibility study, **(b)** Stability study plot and **(c)** Real sample analysis plot.

Chapter 6

Conclusions

This report deals with the results of studies relating to development of a flexible, label free, light weight and disposable electrochemical biosensor. It has been found that PEDOT:PSS and nFe_2O_3 modified paper exhibits improved conductivity, high heterogenous electron transfer rate constant, large surface area and provides a suitable matrix for immobilization of biomolecules. The fabricated nFe_2O_3/DMSO@CP electrode has been used for cancer biomarker (CEA) detection, and is found to be highly sensitive (10.2 μA ng^{-1} mL cm^{-2}) with good linearity in the physiological range 4-25 ng mL^{-1} with a lower detection limit of 0.27 ng mL^{-1} and having shelf storage life upto 34 days. Hence, this platform has immense potential for smart point-of-care devices.

Chapter 7

Future Perspective

Although there is huge potential in a paper as a platform for POC devices, novel modification in fabrication, the analysis techniques are further needed to compete with the conventional analytical techniques performance. One customarily faced limitation of these paper based devices is their low detection range, reproducibility and stability. Additional research associated with the fabrication techniques and the incorporation of materials such as solvents and nanomaterials upon the surface needed to be considered to overcome the limitation discussed above and to design better, more stable devices more proficient of detecting multiple analytes at a high sensitivity. It would be a big challenge not to sacrifice the simplicity and cost advantages of paper-based sensors to achieve such devices.

With the improving methodologies, there could be scope for new application areas as portability options become more viable and with the realization that low-cost paper-based devices can meet the objectives for sensitive and accurate monitoring. The detection of other pathogenic diseases, chemical/biological warfare agents, and monitoring of drugs of abuse are just a few examples of application areas where paper-based sensors may be suitable.

Chapter 8

References

1. http://www.cancerresearchuk.org/health-professional/cancer-statistics/worldwide-cancer
2. Aasmundtveit, K., Samuelsen, E., Inganäs, O., Pettersson, L., Johansson, T., Ferrer, S., 2000. Structural aspects of electrochemical doping and dedoping of poly (3, 4-ethylenedioxythiophene). Synthetic metals 113(1), 93-97.
3. Arena, A., Donato, N., Saitta, G., Bonavita, A., Rizzo, G., Neri, G., 2010. Flexible ethanol sensors on glossy paper substrates operating at room temperature. Sensors and Actuators B: Chemical 145(1), 488-494.
4. Ashizawa, S., Shinohara, Y., Shindo, H., Watanabe, Y., Okuzaki, H., 2005. Polymer FET with a conducting channel. Synthetic metals 153(1), 41-44
5. Blackburn, G.F., Shah, H.P., Kenten, J.H., Leland, J., Kamin, R.A., Link, J., Peterman, J., Powell, M.J., Shah, A., Talley, D.B., 1991. Electrochemiluminescence detection for development of immunoassays and DNA probe assays for clinical diagnostics. Clinical Chemistry 37(9), 1534-1539.
6. Briseno, A.L., Roberts, M., Ling, M.-M., Moon, H., Nemanick, E.J., Bao, Z., 2006. Patterning organic semiconductors using "dry" poly (dimethylsiloxane) elastomeric stamps for thin film transistors. Journal of the American Chemical Society 128(12), 3880-3881.
7. Bloor, D., Movaghar, B., 1983. Conducting polymers. IEE Proceedings I-Solid-State and Electron Devices 130(5), 225-232.
8. Cao, G., 2004. Synthesis, properties and applications. World Scientific.
9. Cao, S.-W., Zhu, Y.-J., Ma, M.-Y., Li, L., Zhang, L., 2008. Hierarchically nanostructured magnetic hollow spheres of Fe3O4 and γ-Fe2O3: preparation and potential application in drug delivery. The Journal of Physical Chemistry C 112(6), 1851-1856
10. Chou, T.-R., Chen, S.-H., Chiang, Y.-T., Lin, Y.-T., Chao, C.-Y., 2015. Highly conductive PEDOT: PSS films by post-treatment with dimethyl sulfoxide for ITO-free liquid crystal display. Journal of Materials Chemistry C 3(15), 3760-3766.
11. Feng, K.-J., Yang, Y.-H., Wang, Z.-J., Jiang, J.-H., Shen, G.-L., Yu, R.-Q., 2006. A nano-porous CeO 2/Chitosan composite film as the immobilization matrix for colorectal cancer DNA sequence-selective electrochemical biosensor. Talanta 70(3), 561-565.

12. Figuerola, A., Di Corato, R., Manna, L., Pellegrino, T., 2010. From iron oxide nanoparticles towards advanced iron-based inorganic materials designed for biomedical applications. Pharmacological Research 62(2), 126-14
13. Gong, S., Schwalb, W., Wang, Y., Chen, Y., Tang, Y., Si, J., Shirinzadeh, B., Cheng, W., 2014. A wearable and highly sensitive pressure sensor with ultrathin gold nanowires. Nature communications 5.
14. Groenendaal, L., Jonas, F., Freitag, D., Pielartzik, H., Reynolds, J.R., 2000. Poly (3, 4-ethylenedioxythiophene) and its derivatives: past, present, and future. Advanced Materials 12(7), 481-494.
15. Heeger, A., Moses, D., Sinclair, M., 1986. Semiconducting polymers: fast response non-linear optical materials. Synthetic metals 15(2-3), 95-104.
16. Hejmadi, M., 2010. Introduction to Cancer Biology. Bookboon.
17. Hyun, W.J., Park, O.O., Chin, B.D., 2013. Foldable graphene electronic circuits based on paper substrates. Advanced Materials 25(34), 4729-4734.
18. Iles, R., Kallichurn, H., 2013. What will be the Future Development of Electrochemical Biosensors for the Detection and Quantification of Biomarkers? Journal of Bioengineering & Biomedical Science 2012.
19. Jang, J., Chang, M., Yoon, H., 2005. Chemical Sensors Based on Highly Conductive Poly (3, 4-ethylenedioxythiophene) Nanorods. Advanced Materials 17(13), 1616-1620.
20. Jeong, C.J., Sharker, S.M., In, I., Park, S.Y., 2015. Iron Oxide@ PEDOT-Based Recyclable Photothermal Nanoparticles with Poly (vinylpyrrolidone) Sulfobetaines for Rapid and Effective Antibacterial Activity. ACS applied materials & interfaces 7(18), 9469-9478.
21. Kim, J., Jung, J., Lee, D., Joo, J., 2002. Enhancement of electrical conductivity of poly (3, 4-ethylenedioxythiophene)/poly (4-styrenesulfonate) by a change of solvents. Synthetic metals 126(2), 311-316.
22. Kirchmeyer, S., Reuter, K., 2005. Scientific importance, properties and growing applications of poly (3, 4-ethylenedioxythiophene). Journal of Materials Chemistry 15(21), 2077-2088.
23. Kongsuphol, P., Ng, H.H., Pursey, J.P., Arya, S.K., Wong, C.C., Stulz, E., Park, M.K., 2014. EIS-based biosensor for ultra-sensitive detection of TNF-α from non-diluted human serum. Biosensors and Bioelectronics 61, 274-279.

24. Kroschwitz, J.I., 1988. Electrical and electronic properties of polymers: a state-of-the-art compendium. Wiley New York.
25. Kumar, S., Willander, M., Sharma, J.G., Malhotra, B.D., 2015. A solution processed carbon nanotube modified conducting paper sensor for cancer detection. Journal of Materials Chemistry B 3(48), 9305-9314.
26. Kumar, S., Sen, A., Kumar, S., Augustine, S., Yadav, B.K., Mishra, S., Malhotra, B.D., 2016. Polyaniline modified flexible conducting paper for cancer detection. Applied Physics Letters 108(20), 203702.
27. Lei, J., Lei, C., Wang, T., Yang, Z., Zhou, Y., 2013. Detection of targeted carcinoembryonic antigens using a micro-fluxgate-based biosensor. Applied Physics Letters 103(20), 203705.
28. Liana, D.D., Raguse, B., Gooding, J.J., Chow, E., 2012. Recent advances in paper-based sensors. Sensors 12(9), 11505-11526.
29. Li, H., Wei, Q., He, J., Li, T., Zhao, Y., Cai, Y., Du, B., Qian, Z., Yang, M., 2011. Electrochemical immunosensors for cancer biomarker with signal amplification based on ferrocene functionalized iron oxide nanoparticles. Biosensors and Bioelectronics 26(8), 3590-3595.
30. Li, H., Wei, Q., Wang, G., Yang, M., Qu, F., Qian, Z., 2011. Sensitive electrochemical immunosensor for cancer biomarker with signal enhancement based on nitrodopamine-functionalized iron oxide nanoparticles. Biosensors and Bioelectronics 26(6), 3044-3049.
31. Liu, F., Zhang, Y., Yu, J., Wang, S., Ge, S., Song, X., 2014. Application of ZnO/graphene and S6 aptamers for sensitive photoelectrochemical detection of SK-BR-3 breast cancer cells based on a disposable indium tin oxide device. Biosensors and Bioelectronics 51, 413-420.
32. Ludwig, J.A., Weinstein, J.N., 2005. Biomarkers in cancer staging, prognosis and treatment selection. Nature Reviews Cancer 5(11), 845-856.
33. Luo, Y., Liu, H., Rui, Q., Tian, Y., 2009. Detection of extracellular H2O2 released from human liver cancer cells based on TiO2 nanoneedles with enhanced electron transfer of cytochrome c. Analytical chemistry 81(8), 3035-3041.
34. Manekkathodi, A., Lu, M.Y., Wang, C.W., Chen, L.J., 2010. Direct Growth of Aligned Zinc Oxide Nanorods on Paper Substrates for Low-Cost Flexible Electronics. Advanced Materials 22(36), 4059-4063

35. Nardes, A.M., Kemerink, M., De Kok, M., Vinken, E., Maturova, K., Janssen, R., 2008. Conductivity, work function, and environmental stability of PEDOT: PSS thin films treated with sorbitol. Organic electronics 9(5), 727-734.
36. Okuzaki, H., Ishihara, M., Ashizawa, S., 2003. Characteristics of conducting polymer transistors prepared by line patterning. Synthetic metals 137(1-3), 947-948.
37. Ouyang, J., Xu, Q., Chu, C.-W., Yang, Y., Li, G., Shinar, J., 2004. On the mechanism of conductivity enhancement in poly (3, 4-ethylenedioxythiophene): poly (styrene sulfonate) film through solvent treatment. Polymer 45(25), 8443-8450.
38. Ouyang, L., Musumeci, C., Jafari, M.J., Ederth, T., Inganäs, O., 2015. Imaging the phase separation between PEDOT and polyelectrolytes during processing of highly conductive PEDOT: PSS films. ACS applied materials & interfaces 7(35), 19764-19773.
39. Pokropivny, V., Skorokhod, V., 2007. Classification of nanostructures by dimensionality and concept of surface forms engineering in nanomaterial science. Materials Science and Engineering: C 27(5), 990-993.
40. Poole Jr, C.P., Owens, F.J., 2003. Introduction to nanotechnology. John Wiley & Sons.
41. Rosa, A.M.D., Kumakura, M., 1995. Trapping method of antibodies on surfaces of polymerizing discs for enzyme immunoassay. Analytica chimica acta 312(1), 85-94.
42. Ruecha, N., Rangkupan, R., Rodthongkum, N., Chailapakul, O., 2014. Novel paper-based cholesterol biosensor using graphene/polyvinylpyrrolidone/polyaniline nanocomposite. Biosensors and Bioelectronics 52, 13-19.
43. Singh, K., Ohlan, A., Saini, P., Dhawan, S., 2008. Poly (3, 4-ethylenedioxythiophene) γ-Fe2O3 polymer composite–super paramagnetic behavior and variable range hopping 1D conduction mechanism–synthesis and characterization. Polymers for Advanced Technologies 19(3), 229-236.
44. Solanki, P.R., Kaushik, A., Agrawal, V.V., Malhotra, B.D., 2011. Nanostructured metal oxide-based biosensors. NPG Asia Materials 3(1), 17-24.
45. Szturmowicz, M., Tomkowski, W., Fijalkowska, A., Sakowicz, A., Filipecki, S., 1995. 1268 Is an increased carcinoembryonic antigen (CEA) concentration in pericardial fluid an indication of malignant pericarditis? European Journal of Cancer 31, S264.

46. Tartaj, P., del Puerto Morales, M., Veintemillas-Verdaguer, S., González-Carreño, T., Serna, C.J., 2003. The preparation of magnetic nanoparticles for applications in biomedicine. Journal of Physics D: Applied Physics 36(13), R182.
47. Wang, J., Lu, C., Chu, K., Ma, C., Wu, D., Tsai, H., Yu, F., Hsieh, J., 2007. Prognostic significance of pre-and postoperative serum carcinoembryonic antigen levels in patients with colorectal cancer. European Surgical Research 39(4), 245-250.
48. Wang, L., Chen, W., Xu, D., Shim, B.S., Zhu, Y., Sun, F., Liu, L., Peng, C., Jin, Z., Xu, C., 2009. Simple, rapid, sensitive, and versatile SWNT− paper sensor for environmental toxin detection competitive with ELISA. Nano letters 9(12), 4147-4152.
49. Wei, Q., Xiang, Z., He, J., Wang, G., Li, H., Qian, Z., Yang, M., 2010. Dumbbell-like Au-Fe 3 O 4 nanoparticles as label for the preparation of electrochemical immunosensors. Biosensors and Bioelectronics 26(2), 627-631.
50. Wu, Y., Li, Y., Ong, B.S., 2007. A simple and efficient approach to a printable silver conductor for printed electronics. Journal of the American Chemical Society 129(7), 1862-1863.
51. Wu, W., Xiao, X., Zhang, S., Zhou, J., Fan, L., Ren, F., Jiang, C., 2010. Large-scale and controlled synthesis of iron oxide magnetic short nanotubes: shape evolution, growth mechanism, and magnetic properties. The Journal of Physical Chemistry C 114(39), 16092-16103.
52. Yager, P., Edwards, T., Fu, E., Helton, K., Nelson, K., Tam, M.R., Weigl, B.H., 2006. Microfluidic diagnostic technologies for global public health. Nature 442(7101), 412-418.
53. Yan, H., Kagata, T., Mori, Y., Harashina, Y., Hara, Y., Okuzaki, H., 2008. Micrometer-scaled channel lengths of organic field-effect transistors patterned by using PEDOT/PSS microfibers. Chemistry Letters 37(1), 44-45.
54. Yuan, J., Wang, G., Majima, K., Matsumoto, K., 2001. Synthesis of a terbium fluorescent chelate and its application to time-resolved fluoroimmunoassay. Analytical chemistry 73(8), 1869-1876.
55. Zhang Y, Kohler N, Zhang M (2002) Surface modification of superparamagnetic magnetite nanoparticles and their intracellular uptake. Biomaterials 23:1553–1561
56. Zhao, W., Ali, M.M., Aguirre, S.D., Brook, M.A., Li, Y., 2008. Paper-based bioassays using gold nanoparticle colorimetric probes. Analytical chemistry 80(22), 8431-8437.